

Polyphase deformation history and strain analyses of the post-amalgamation depositional basins in the Arabian–Nubian Shield: Evidence from Fatima, Ablah and Hammamat Basins



Zakaria Hamimi ^{a,*}, Abdelhamid El-Fakharani ^{a,b}, Mamdouh M. Abdeen ^c

^a Department of Structural Geology and Remote Sensing, Faculty of Earth Sciences, King Abdulaziz University, Jeddah, Saudi Arabia

^b Geology Department, Faculty of Science, Aswan University, Egypt

^c National Authority for Remote Sensing and Space Sciences (NARSS), Egypt

ARTICLE INFO

Article history:

Available online 17 October 2013

Keywords:

Arabian–Nubian Shield
Fatima Basin
Ablah Basin
Hammamat Basin
Polyphase deformation
Strain analysis

ABSTRACT

Post-amalgamation depositional basins <650 Ma (PADBs), dominated by volcano–sedimentary assemblages, unconformably overlying Neoproterozoic juvenile (mantle-derived) arcs, represent one of the main collage in the Arabian–Nubian Shield (ANS). In this work, three distinguished PADBs; namely Fatima, Ablah and Hammamat PADBs, are the subject matter of detailed field investigations and quantitative strain analysis in an attempt to highlight the polyphase deformation history of these PADBs and to discern whether the ANS's PADBs were deformed at the same time or not. The Fatima PADB is studied in its type locality along the northwestern flank of Wadi Fatima; between Jabal Abu Ghurrah and Jabal Daf, in Jeddah tectonic terrane. The Ablah PADB is examined around Wadi Yiba, further south of its type locality near Jabal Ablah in Al-Aqiq Quadrangle, in Asir tectonic terrane. The Hammamat PADB is investigated in Wadi Umm Gheig, Wadi Allaqi and Wadi Hodein in the Egyptian Eastern Desert tectonic terrane. It is supposed that the Fatima is a basin controlled by dextral transcurrent shearing occurred along the NE-oriented Wadi Fatima Shear Zone and the Ablah is a strike-slip pull-apart basin, and both basins were believed to be deposited during and soon after the Nabitah Orogeny (680–640 Ma) that marked suturing of the Afif terrane with the oceanic ANS terranes to the west. They were affected by at least three Neoproterozoic deformation phases and show geometric and kinematic relationships between folding and thrusting. The Hammamat PADB is a fault-bounded basin affected by a NW–SE- to NNW–SSE-oriented shortening phase just after the deposition of the molasse sediments, proved by NW- to NNW-verging folds and SE- to SSE-dipping thrusts that were refolded and thrust in the same direction. The shortening phase in the Hammamat was followed by a transpressional wrenching phase related to the Najd Shear System, which resulted in the formation of NW–SE sinistral-slip faults associated with positive flower structures that comprise NE-verging folds and SW-dipping thrusts. Strain results in the three studied PADBs are nearly consistent, indicating that they are correlated and underwent the same history of deformation. The ANOVA test indicates that there is no significant difference for the Vector mean and I_{SYM} for the three PADBs. There is only a significant difference for the Harmonic mean (P -value < 0.05). A Post Hoc test (Shefee) shows that the difference exists between the Allaqi and the Umm Gheig's deformed poly-mictic conglomeratic pebbles of the Hammamat PADB.

© 2013 Elsevier Ltd. All rights reserved.

1. Introduction

Some forty post-amalgamation depositional basins (PADBs) are known in the ANS (Fig. 1). These PADBs are sporadically distributed and each of which ranging in area from about 200 km² to 72,000 km²; the largest PADB at all is the Murdama PADB in the

northeastern ANS (e.g., Johnson, 2003; Matsah and Kusky, 1999, 2001; Willis et al., 1988; Johnson and Woldehaimanot, 2003; Abdeen and Greiling, 2005; Eliwa et al., 2006, 2010; Hamimi et al., 2012a,b). The PADBs comprise slightly to moderately metamorphosed, and at the same time variably deformed, volcanosedimentary successions that were deposited after 650 Ma over newly amalgamated arc terranes (Johnson et al., 2011). They are frequently structurally-controlled (fault-controlled down sags, pull aparts, rifts, half-grabens, thrusting, normal faulting, magmatic

* Corresponding author. Tel.: +966 501870196.

E-mail address: yahiahamimi@gmail.com (Z. Hamimi).

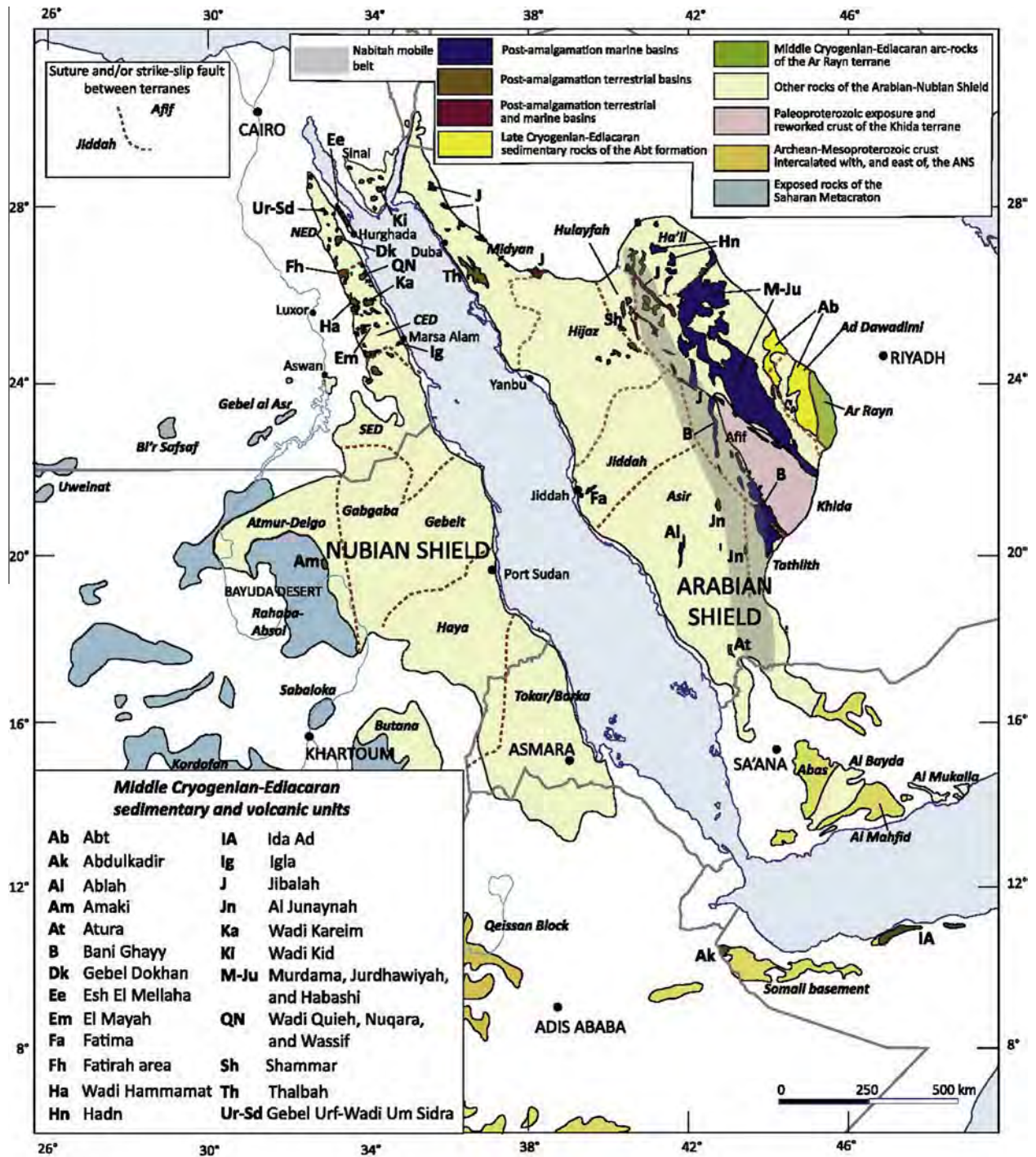


Fig. 1. Simplified map of the ANS tectonostratigraphic terranes showing the Middle Cryogenian–Ediacaran sedimentary and volcanic assemblages that are mostly cropping out in PADDs, unconformable on newly amalgamated arc terranes. Exceptions are the Abt formation (Ab) and the arc rocks of the Ar Rayn terrane, which were treated as late Cryogenian–Ediacaran terranes rather than PADDs (after Johnson et al., 2011).

doming, etc.) (e.g. Abdeen and Greiling, 2005; Shalaby et al., 2006; Alsubhi, 2012); some PADDs were classified as foreland and intermontane basins (e.g. Fritz et al., 1996; Abd El-Wahed, 2010; Hamimi et al., 2012b). The PADDs are autochthonous as indicated by their unconformable basal contacts vs. older basement rocks. Johnson and Woldehaimanot (2003) discriminated the PADDs into marine and terrestrial basins, together with mixed terrestrial–marine basins based on their carbonate succession, relative abundances

of grey–green and red–purple rocks and other sedimentary structures. Marine post-amalgamation basins (MPADDs), typified by the Murdama, Bani Ghayy, Fatima and Ablah Groups, are prominent in the eastern part of the ANS. These PADDs began to be deposited during and soon after the Nabatah orogeny (680–640 Ma) that marked suturing of the Afif terrane with the oceanic ANS terranes to the west (Johnson et al., 2011). The Allaqi PADD in southeastern Egypt includes shelf related-sediments of yellow and

blue silica marble (El Gaby and Greiling, 1988). The Allaqi marble is exposed as thrust sheets stacked with chlorite–amphibolite schist, quartz–biotite–garnet schist and gneiss (Abdeen and Abdelghaffar, 2011). In the present study, we believe that the Allaqi PADB may be correlated with the Ablah PADB in the Arabian Shield due to similarities in composition and in the structural setting. Terrestrial post-amalgamation basins (TPADBs), typified by Thalbah PADB (100 km by 45 km) in the Midyan terrane (e.g. Davies, 1985) and the Hammamat PADB in the Eastern Desert of Egypt (e.g. Akaad and El Ramly, 1958; El Ramly, 1972; Grothaus et al., 1979; Wilde and Youssef, 2000; Breitzkreuz et al., 2010), were filled by molasse-type sediments interfingering with subordinate to predominant amounts of volcanic rocks. The molasse-type sediments imply external and internal syn- to late orogenic foreland and intermontane basins respectively; that are collapsed and underwent extensional and strike-slip faulting (Johnson et al., 2011). The terrestrial marine post-amalgamations basins (TMPADBs) are manifested by the Jibalah Group that crops out in small, isolated synclinal basins neighboring the NW-trending Najd Fault System in the northern part of the Arabian Shield (Delfour, 1970).

Although the PADBs in the ANS have been the issue of numerous respectable studies, “fundamental unanswered questions arise, including: (1) the causes of subsidence that created the basins, whether thermal contraction, loading or flexure downwarping, or extension and pull-apart development in strike slip systems; (2) the apparent genetic relationships between basin formation and local and regional structures such as strike-slip faulting and mantle doming; (3) the relationship between basin formation and granitoid magmatism; (4) the extent to which some of the basins were originally interconnected; (5) which basins were marine or connected to a late Cryogenian–Ediacaran ocean; and (6) whether any basins contain unequivocal Ediacaran multicellular fossils” (Johnson et al., 2011). The present work presents the results of detailed field-structural investigation carried out on three outstanding PADBs; specifically Fatima, Ablah and Hammamat PADBs. The main goal of this study is to add much more insights into the wealth of data gathered from the PADBs, and this is consequently may contribute to the tectonic setting and deformational history of such basins that represent one of the main pillars in the ANS’s Precambrian geology.

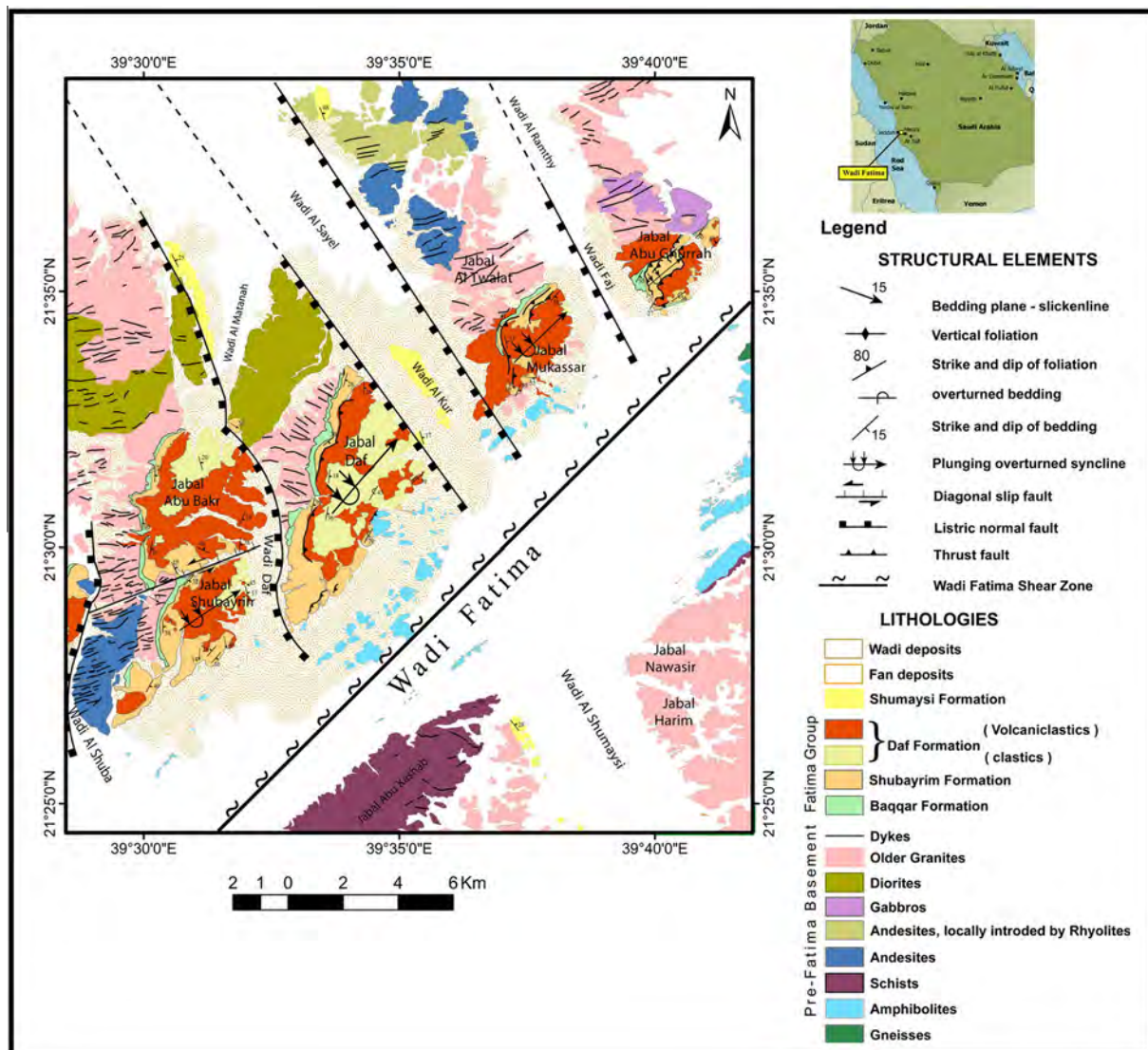


Fig. 2. Detailed geologic map of the area bounded by long. 39°28'24.06" and 39°42'2.457"E and lat. 21°24'49.67" and 21°39'4.11"N showing the majority of the NE-oriented FPADB (after Al-Gabali, 2012; Hamimi et al., 2012c).

2. Geologic setting

2.1. Fatima Basin

Fatima Post-amalgamation Depositional Basin (FPADB) is a NE-oriented basin in Jeddah tectonic terrane, extending over ~33 km (maximum width 8 km) along the western flank of the main Wadi Fatima, from Jabal Abu Ghurrah in the northeast to Jabal Shilwa and Jabal Al-Ujaysah in the southwest (Fig. 2). In this PADB, the volcanosedimentary succession of the Fatima Group rests unconformably over the pre-Fatima older basement suite (Fig. 3a) which represented mainly by gneisses, amphibolites, schists, andesites locally intruded by rhyolites, gabbros, diorites and older granites (773 ± 16 Ma old, Rb/Sr whole rock age; Duyverman et al., 1982). The unconformable basal contact is marked by a polymictic conglomeratic bed reaching up to 20 m thick (Fig. 3b). Such type of geologic contact reveals that the volcanosedimentary succession is autochthonous, in place at its site of deposition. The Fatima Group attains its maximum thickness (~450 m) in Jabal Daf and Jabal Abu Bakr. It is represented by a series of well-bedded sandy, silty and calcareous sediments, with intercalated andesitic flows and sills (Fig. 3c), in which three units are distinguished (Nebert

et al., 1974): (a) Lower clastic unit; a clastic sedimentary sequence of sandstones and siltstones with a predominantly greenish color, (b) Middle carbonate unit; consisting of limestones, sandy limestones and marbles of a predominantly yellowish white color, with abundant crypogalaminates, stromatolites (Fig. 3d), and archeocyathid biomicrites that may have been deposited in a stable shallow littoral–marine platform (Basahel et al., 1984), and (c) Upper clastic unit; consisting of a lower siltstone member and an upper pyroclastic member, with an overall reddish color. Polymictic conglomerates are well recognized in the upper clastic unit of the Fatima Group (Fig. 3e and f). Moore and Al-Rehaili (1989) gave the name “Fatima Group” and classified it into three formations (from top to base); Daf Formation, Shubayrim Formation and Baqqar Formation. Detailed description of the three formations was given by Nebert et al. (1974), Al-Gabali (2012) and Hamimi et al. (2012b). However, Fig. 4 is a tentative stratigraphic section of Fatima Group volcanosedimentary sequence.

2.2. Ablah Basin

Ablah Post-amalgamation Depositional basin (APADB) is a N-oriented basin in the northwestern part of the Asir tectonic terrane.

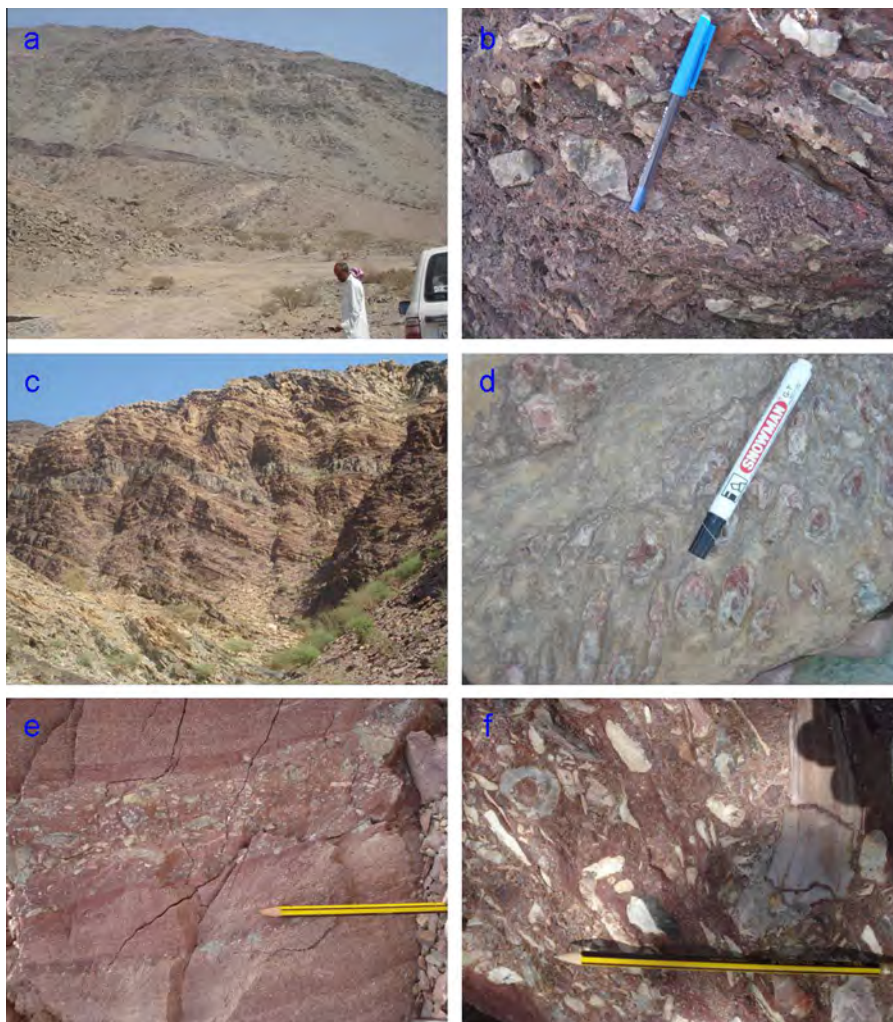


Fig. 3. Field photographs of the Fatima volcanosedimentary sequence. (a) Unconformable contact of the Fatima Group versus the newly amalgamated arc rocks. (b) Oriented deformed polymictic conglomerates. (c) An andesitic sill extruded near the contact between the lower clastic unit (Daf Formation) and the middle carbonate unit (Shubayrim Formation) of the Fatima Group; the sill exhibits the same deformation of the Fatima Group. (d) Ferruginated, silicified stromatolitic carbonate oncoids. (e and f) Polymictic conglomerates recorded within the upper clastic unit (Baqqar Formation) of the Fatima Group.

It
o-
c-
c-
u-
p-
i-
es
a
p-
a-
r-
t
of
A-
l-
A-
q-
iq
Q-
u-
a-
d-
r-
a-
n-
g-

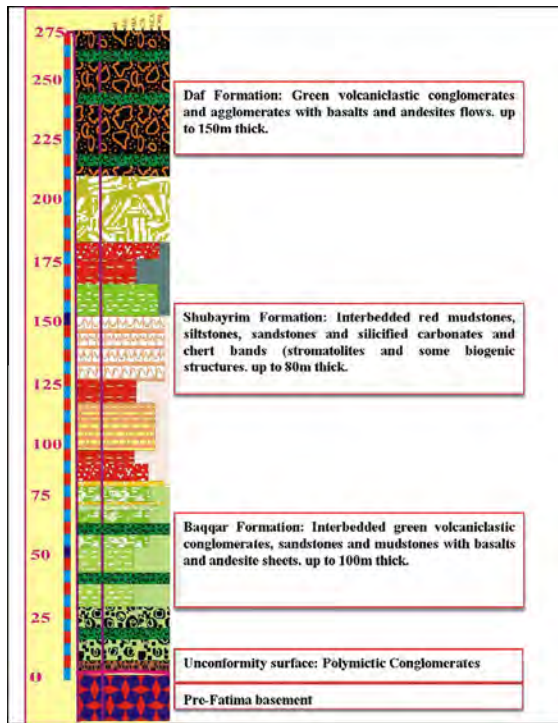


Fig. 4. Tentative stratigraphic section of Fatima Group volcanosedimentary sequence.

le. The boundary between Ablah Group and the juvenile arc rocks of Asir terrane is delineated by the Umm Farwah Shear Zone (UFSZ) that extends about 200 km N–S across the Arabian Shield (Fig. 5). The UFSZ developed in the early Cryogenian terrane of arc-related volcanosedimentary and plutonic rocks mixed with discrete large lenses of serpentinite in a typical mélangé sequence (Moufti, 2001; Johnson et al., 2011). Near Jabal Ablah, the type section of Ablah Group, previous investigators (e.g. Zakir, 1972; Greenwood, 1975; Donzeau and Benzait, 1989) subdivided the exposed Neoproterozoic basement rocks into two N-striking lithostratigraphic complexes; (1) a volcanic and volcanoclastic complex to the east comprising the Jeddah Group and (2) a detrital volcanosedimentary complex in the west comprising the Ablah Group. Both groups are separated by serpentinite-decorated major faults. The Jeddah Group is discriminated into two formations; the Qirshah Formation (pyroclastics) and the Khutnah Formation (volcanosedimentary and epiclastic). The Ablah Group comprises three formations; the Rafa, the Jerub and the Thurat Formations, and was believed to be crop out in a tectonic trough or graben (Zakir, 1972; Greenwood, 1975; Donzeau and Benzait, 1989). However, the relationships between the Ablah Group Formations themselves, as well as between the Ablah and the Jeddah Groups were and still are controversial. Following Sanders's et al. (1980), Kattu (2011) subdivided the Ablah Group in Wadi Yiba (Fig. 6) into four main lithologic units; lower clastic-, lower marble-, upper clastic-, and upper marble-units. Detailed description of these units was given

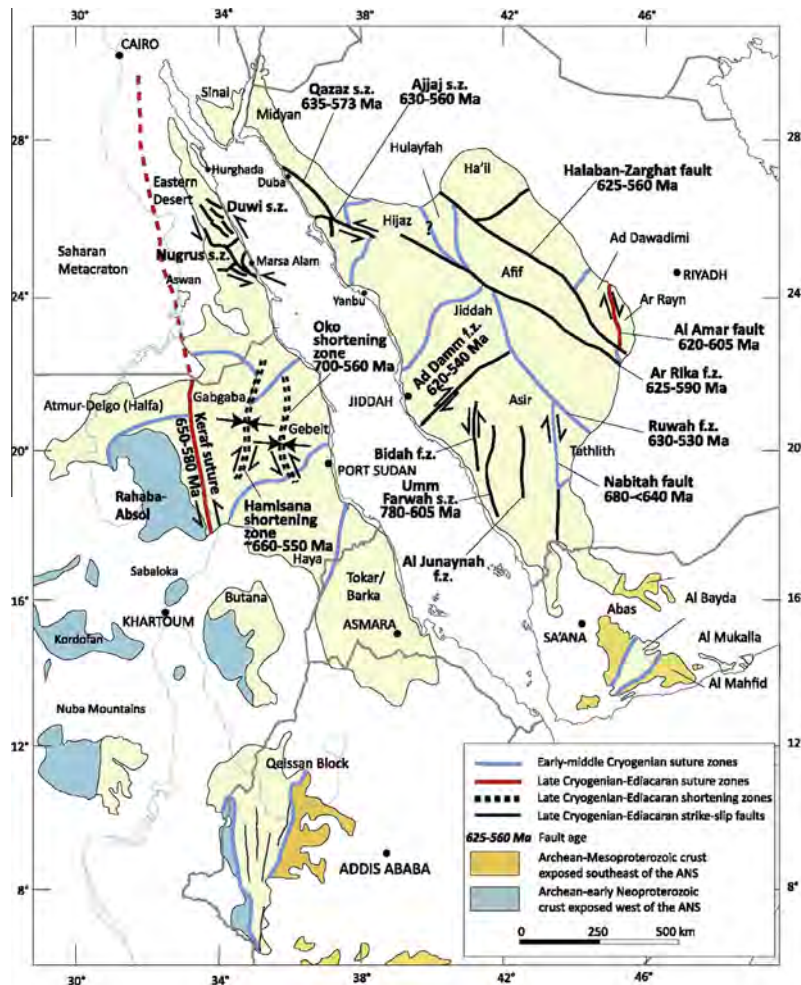


Fig. 5. ANS late Cryogenian–Ediacaran shear zones, shortening zones and sutures (after Johnson et al., 2011). The N–S oriented UFSZ, that represents the boundary between Ablah Group and the juvenile arc rocks of Asir terrane, is observed.

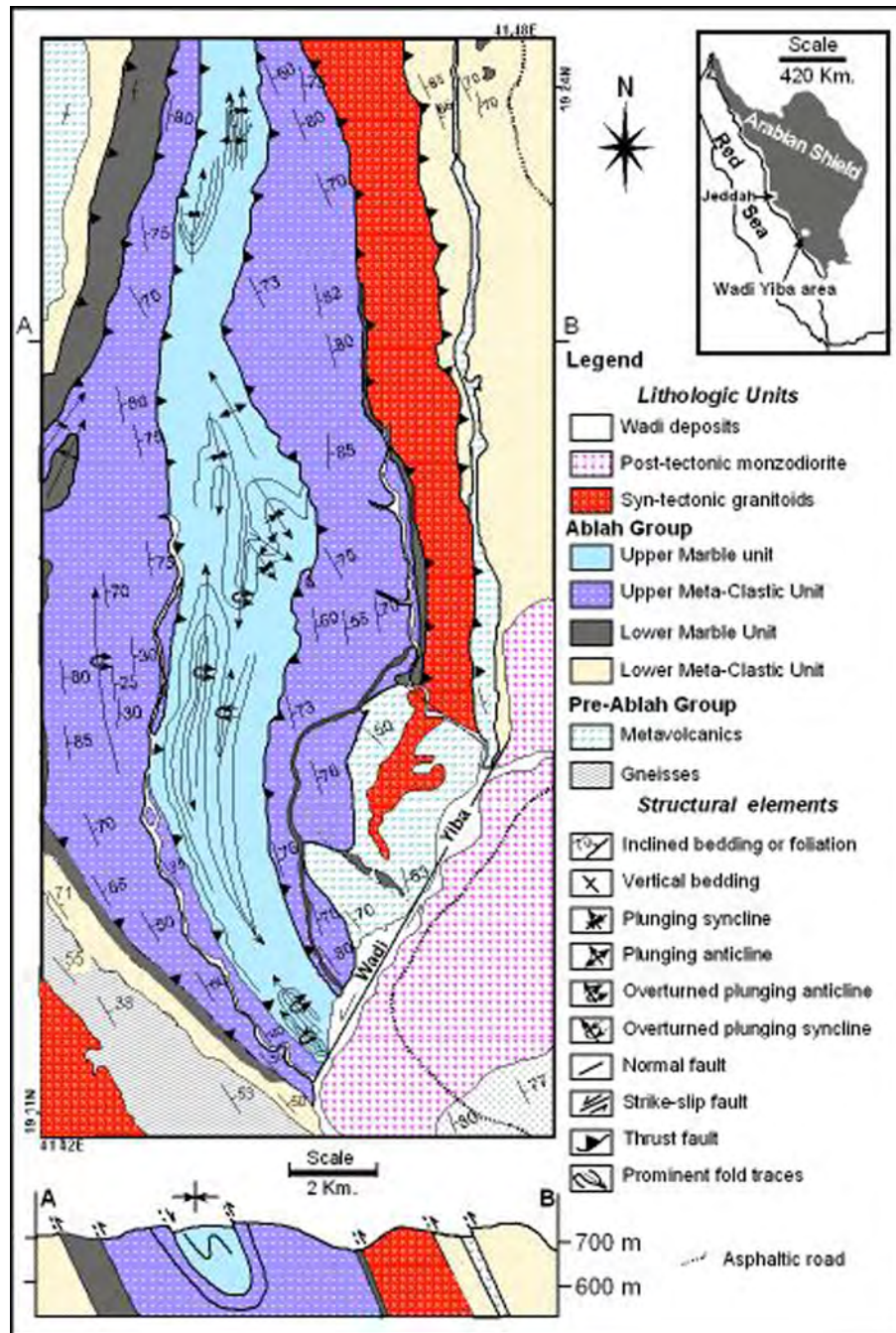


Fig. 6. Detailed geologic map showing the Ablah Group subdivisions around Wadi Yiba; lower clastic-, lower marble-, middle clastic-, and upper marble-units (after Kattu, 2011; Hamimi et al., 2012b).

by Hamimi et al. (2012a). The lower clastic unit consists of sandstone grading into siltstone, and is interpreted to be of deltaic deposits. This unit has a basal conglomerate that contains matrix-supported cobbles of granite and pebbles of andesitic and rhyolitic lavas in a muddy micaceous, ankeritic matrix with epidote and amphibolite. Clasts are well-deformed as they are highly elongated and stretched whose longest axes are oriented parallel to strike of the beds that range in thickness from 2 to 40 m in thickness (Fig. 7a). The lower marble consists of fine-grained siliceous marble interbedded with bands of chlorite schist, calcareous schist and quartz–biotite schist (Fig. 7b). This unit frequently commences with arenite or rudite rapidly giving way up sequence to gray,

green sandy siltstone, and then impure carbonates intercalated with siltstone and finally relatively pure carbonates. The environment of deposition was most probably shallow-water, intertidal to subtidal, as shown by the presence of flaser bedding, oscillation ripples and algal structures. The upper metaclastic unit shows evidence of rapid deposition. In the western part of the area, a typical succession consisting of alternating metamorphosed shale, sandstone, grit and conglomerate is encountered. Crenulation foliation (Strain-slip cleavage) is recognized in this unit (Fig. 7c). The upper marble unit occupies the central part of the study area and exhibits tectonic contact against to the upper metaclastic unit exposed in both eastern and western sides. This unit consists predominantly

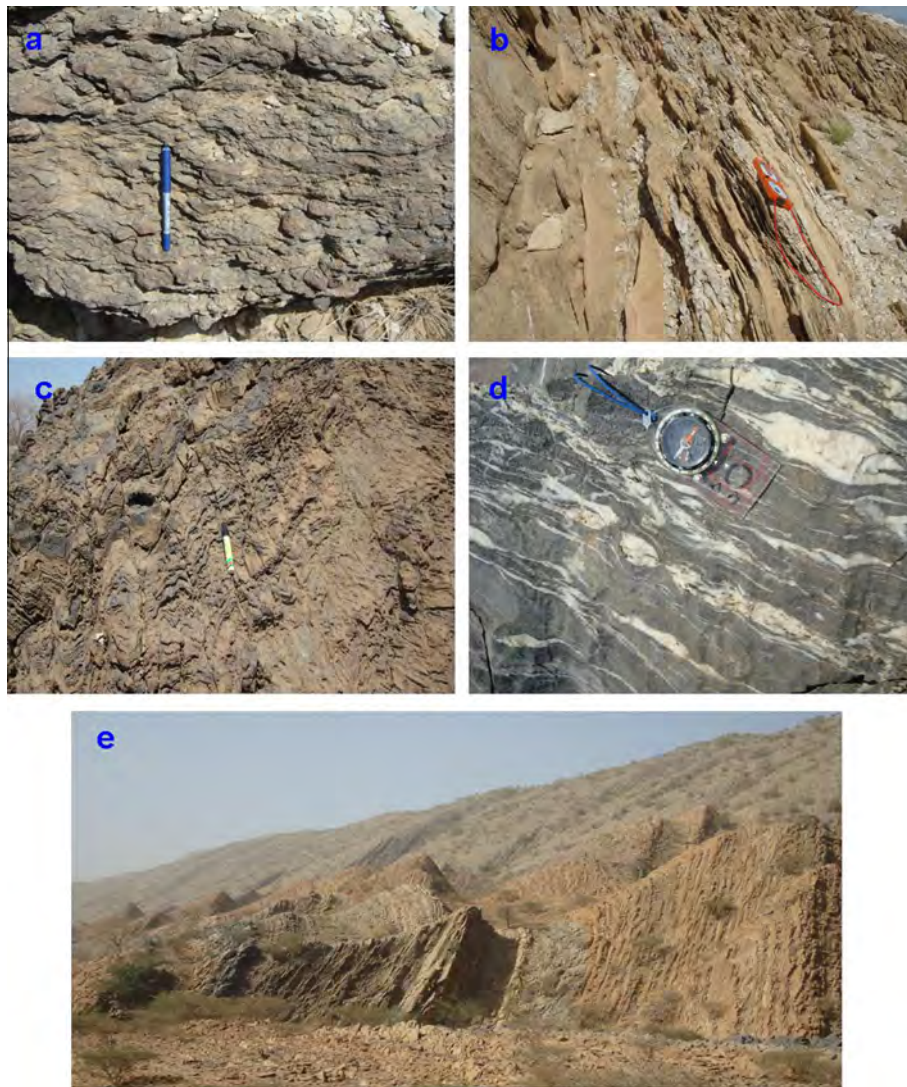


Fig. 7. Field photographs of the Ablah volcanosedimentary sequence. (a) Polymictic conglomerates recorded at the base of the lower metaclastic unit. (b) Remarkable foliation in the lower marble unit. (c) Crenulation foliation (Strain-slip cleavage) in the upper metaclastic unit. (d) Migmatized and boudinaged upper marble unit. (e) Imbricated thrust sheets in the lower part of the Ablah Group.

of buff to white color, fine grained siliceous marble, analogous to that of the lower marble unit, intercalated with minor siltstone and sandy carbonate beds. It exhibits well developed migmatization and boudinage structure (Fig. 7d). A layer of black to gray, fine grained argillaceous marble (up to 25 m thick) and persistent over strike distances of over 22 km, is highly deformed developing isoclinal and overturned parasitic folds with hinges plunging north and south. Fig. 7e shows imbricated thrust sheets in the lower part of the Ablah Group.

2.3. Hammamat Basin

The name Hammamat sediments is after the type locality in Wadi El Hammamat in the northern Eastern Desert of Egypt. The Hammamat sediments are molasse-type sedimentary rocks deposited late to post Pan-African Orogeny (Abdeen and Greiling, 2005). These sediments are exposed sporadically within isolated basins in the Eastern Desert territory (Fig. 8). These basins are of different shapes, although they commonly mostly extend in NW–SE and N–S directions (Rice et al., 1993; Abdeen and Greiling, 2005). The sedimentary section of the Hammamat sediments in the type local-

ity attains a thickness of about 4000 m and composed of polymictic conglomerates, gritstone, sandstone, siltstone, claystone and rare limestone intercalated with volcanoclastic layers (Akaad and Noweir, 1969, 1980). Primary sedimentary structures (e.g. ripple marks, rain-drop prints, mud crack polygons and graded-bedding) are preserved in the Hammamat sediments (Abdeen et al., 1997). The Hammamat sediments have been deposited in three main types of basins (Abd El-Wahed, 2010) including foreland, intermontane (El Gaby et al., 1990), and strike slip basins (Fritz and Messner, 1999). They were deposited by alluvial fan and braided stream systems in intermontane (Grothaus et al., 1979) and foreland basins (El-Gaby et al., 1988) formed during the late stage of the Pan-African orogeny. The basins were formed as down faulted grabens trending NE–SW (Stern et al., 1988) or as pull-apart sags due to NW–SE wrenching (Fritz and Messner, 1999). The Hammamat sediments were deposited in late Precambrian after the eruption of subduction-related Dokhan Volcanics of andesitic to rhyolitic composition (Eliwa et al., 2006) and prior to the emplacement of the post-orogenic granitoides (Akaad and Noweir, 1980).

Sedimentary rocks pertaining to the PADB exposed in Umm Gheig, Allaqi and Hodein areas in the Eastern Desert of Egypt are

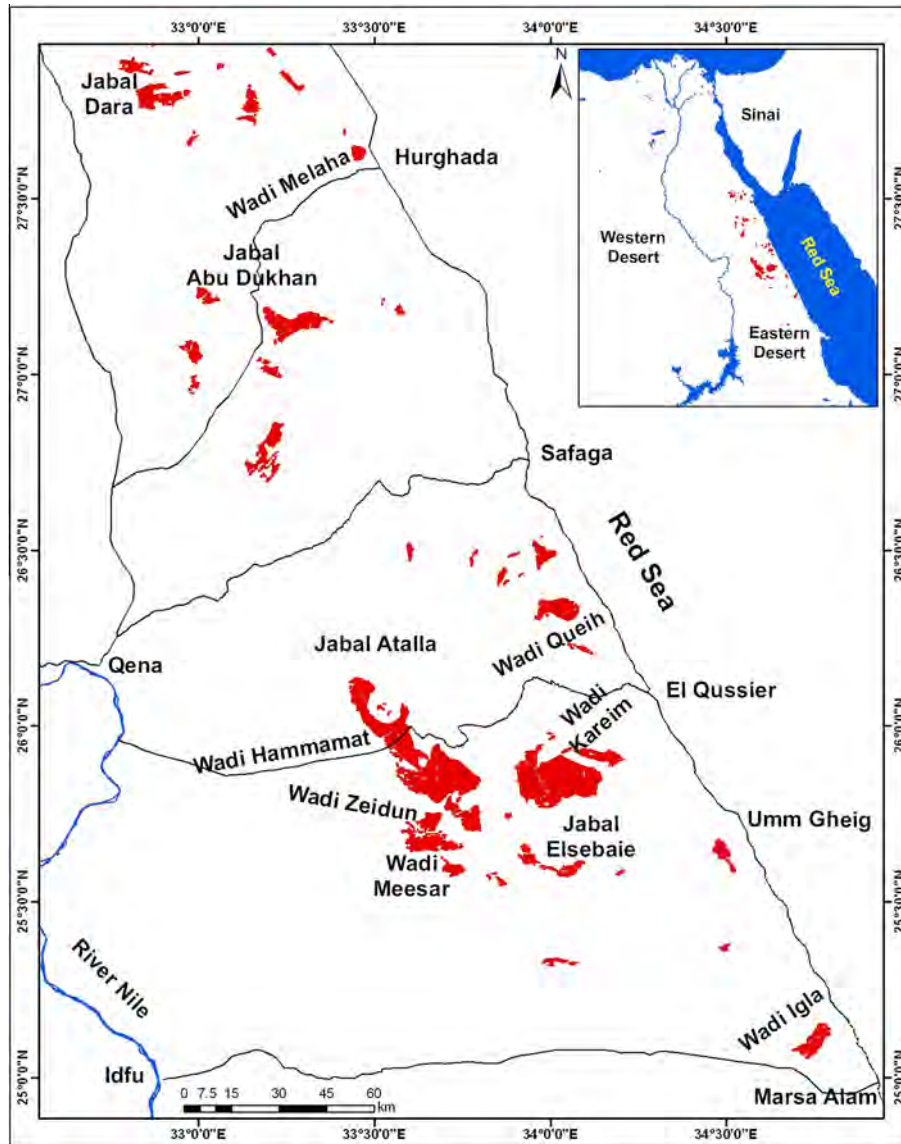


Fig. 8. Distribution of the Hammamat Group small isolated basins in the Eastern Desert of Egypt.

selected to perform detailed structural investigations and strain analysis for subsequent correlation of various post-tectonic sedimentary basins in the ANS. These areas are selected due to presence of conglomeratic pebbles that give good strain markers. They also represent a wide spatial distribution. In the Umm Gheig area, the PADB is represented by the molasse-type Hammamat sedimentary rocks of the Wadi Kareem basin. The sediments are exposed in the north-western part of the Umm Gheig area. They are intruded by Hamrat Ghannam and Nusla late-tectonic granites (Abdeen, 2003). Both the Hammamat sedimentary rocks and the granites are affected by NW–SE trending folds and high angle reverse oblique-slip faults (Fig. 9). Folds are verging towards NE indicating post-Hammamat top to NE tectonic transportation.

In the Allaqi area, the PADB (Abdeen and Abdelghaffar, 2011) are represented by light yellow and blue silica marble associated with thin conglomeratic layers exposed in the western and eastern parts of the Wadi Himur (see Abdeen and Abdelghaffar, 2011 and Fig. 10) as elongated belts. In the western part, thrust sheets strike WNW–ESE for about 15 km; and they show intercalations of marble with acidic metavolcanics and serpentinites. These thrust sheets are folded along WNW–ESE oriented fold axis. In the eastern part, marbles form thrust sheets associated with amphibolites and gneis-

ses that are folded by NNW–SSE trending fold hinges (Abdeen and Abdelghaffar, 2011). The longest exposure is located to the east of Wadi Himur that extends for ca. 5 km long NNE–SSW oriented belt. Other exposures exist as small outcrops along the western side of Wadi Al Biyam. Contacts between marbles and the neighboring rock units structural, therefore genetic relationship with these rock units could not be judged (Abdeen and Abdelghaffar, 2011).

In the Hodein area at the eastern part of the south Eastern Desert of Egypt, the PADB (Abdeen et al., 2008) are composed of conglomerates and acidic volcanics, which exposed in a thrust zone south of Jabal Harhagit (Fig. 11). The pebble longest axis of strained pebbles plunges SSE and its monoclinic asymmetry of pressure shadows indicate top-to-the-SSE transport (Abdeen et al., 2008). However, Fig. 12 shows the Hammamat polymictic conglomerates in the studied areas.

3. Deformation pattern

3.1. Deformation pattern in Fatima Basin

In order to understand the deformation pattern in the Fatima Group, it is better to shed some light on the geologic structures

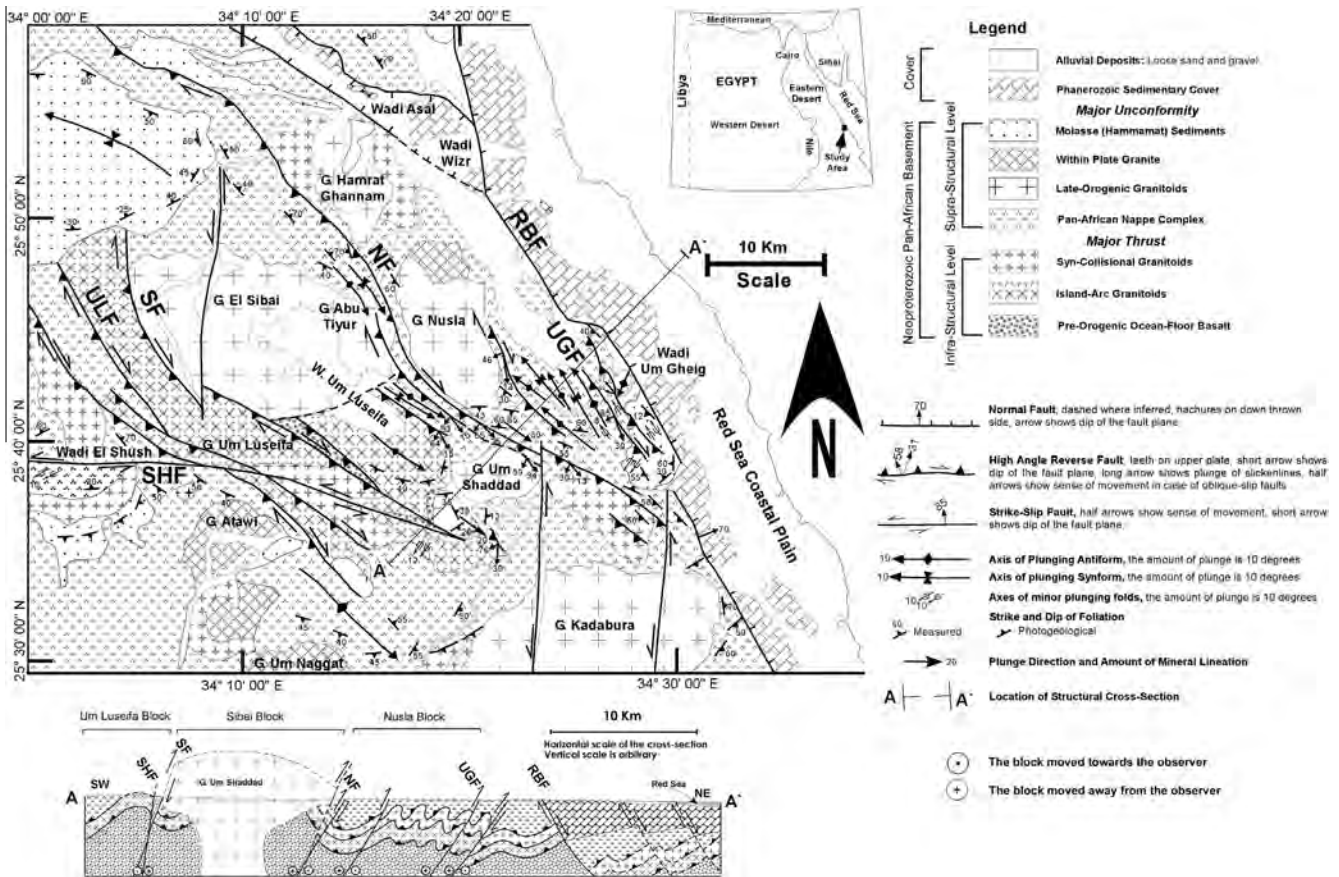


Fig. 9. Geological map and structural cross-section of Um Gheig area (G., Gebel; W., Wadi; RBF, rift-bounding fault; UGF, Um Gheig fault; NF, Nusta fault; SF, Sibai fault; ULF, Um Luseifa fault; SHF, El Shush fault).

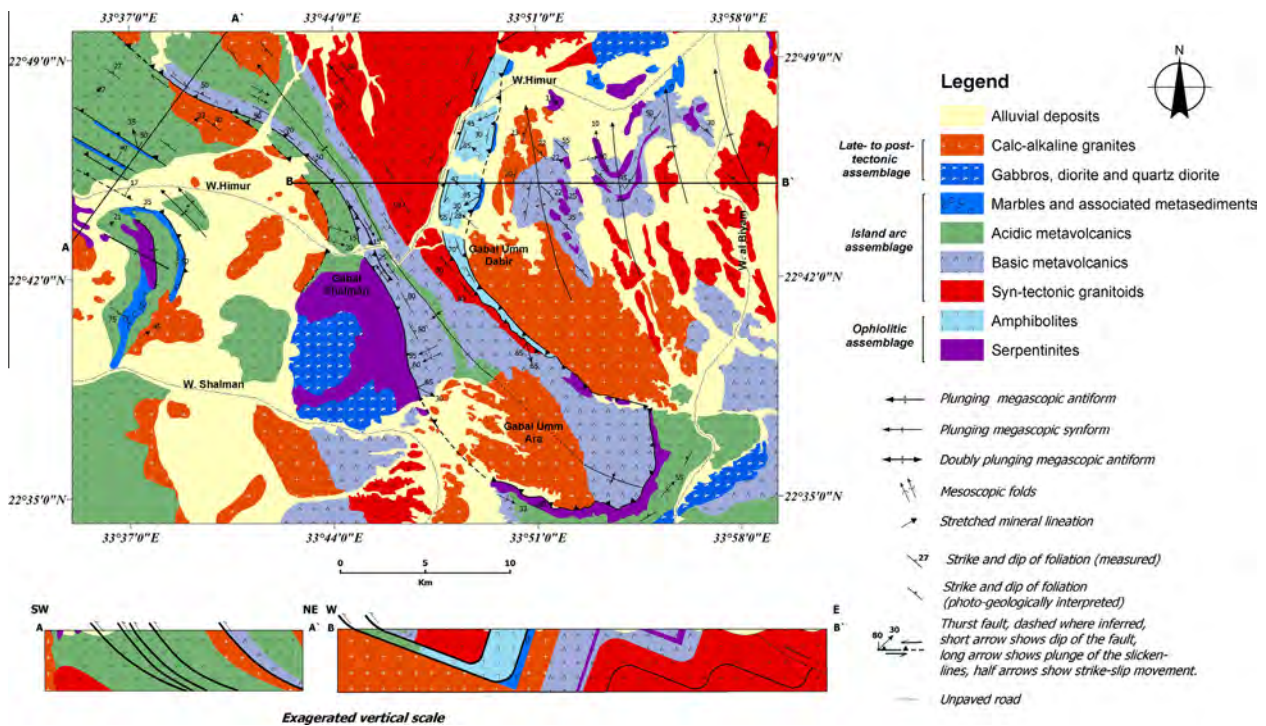


Fig. 10. Detailed geologic map of Allaqi area.

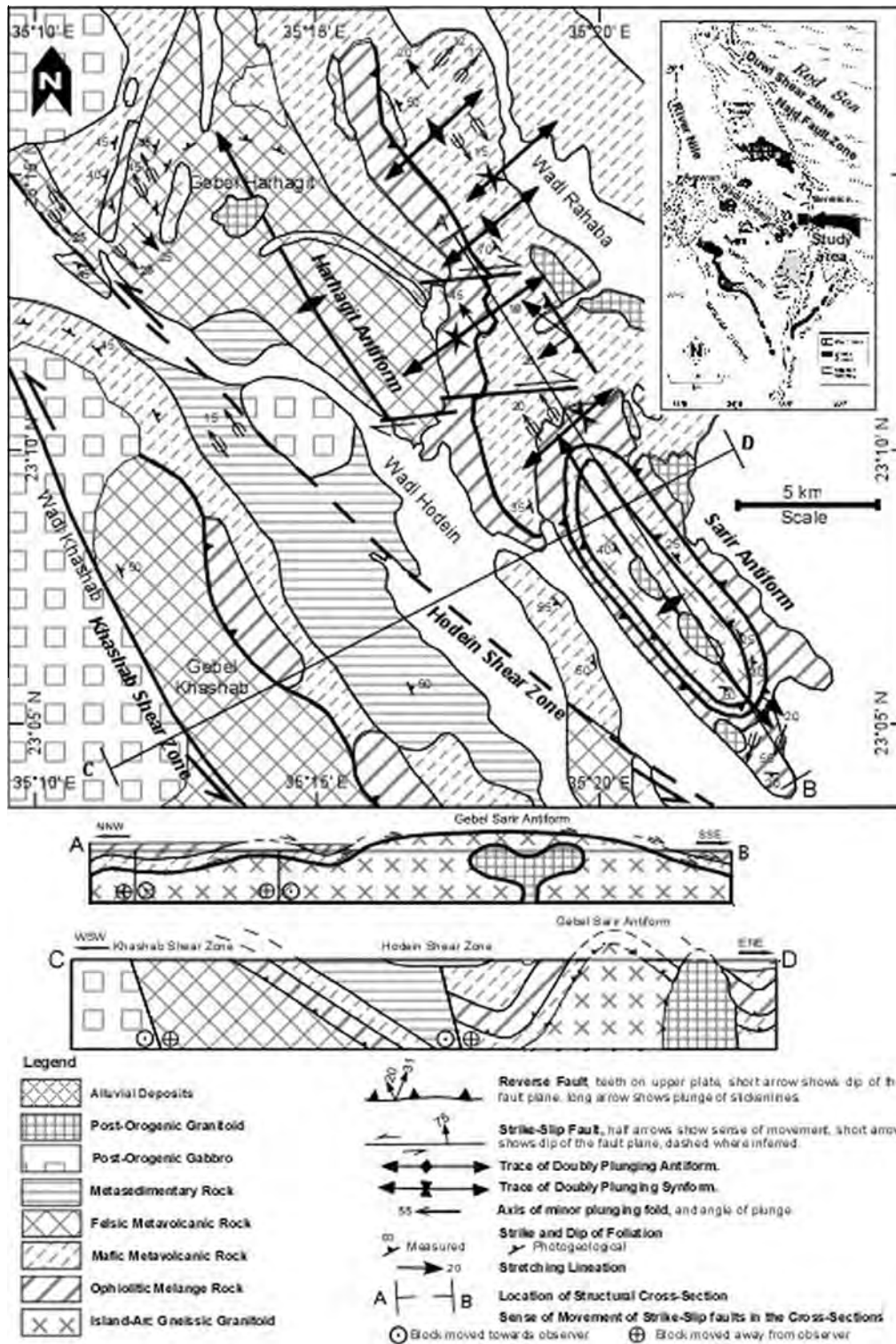


Fig. 11. Detailed geologic map of Hodein area.

recorded below the unconformable basal contact within the pre-Fatima basement rocks, particularly within the remarkably deformed amphibolites and schists. The structures within pre-Fatima basement are typified by attenuated tight isoclinal folds, sheared-out hinges, shear fabrics, tension gashes and tightly appressed fold closures, together with NE–SW foliation planes and subhorizontal stretched and mineral lineations. These structural

fabrics are genetically related to an oldest prominent dextral shearing phase affected the main Wadi Fatima during the Neoproterozoic, pre-dating the deposition of the Fatima Group over the juvenile arc-related rocks; i.e. they are shear zone-related structures. Dextral shearing along Wadi Fatima Shear Zone (WFSZ) is indicated by sigmoidal kinematic indicators with monoclinic symmetry that are encountered at the outcrop scale and observed

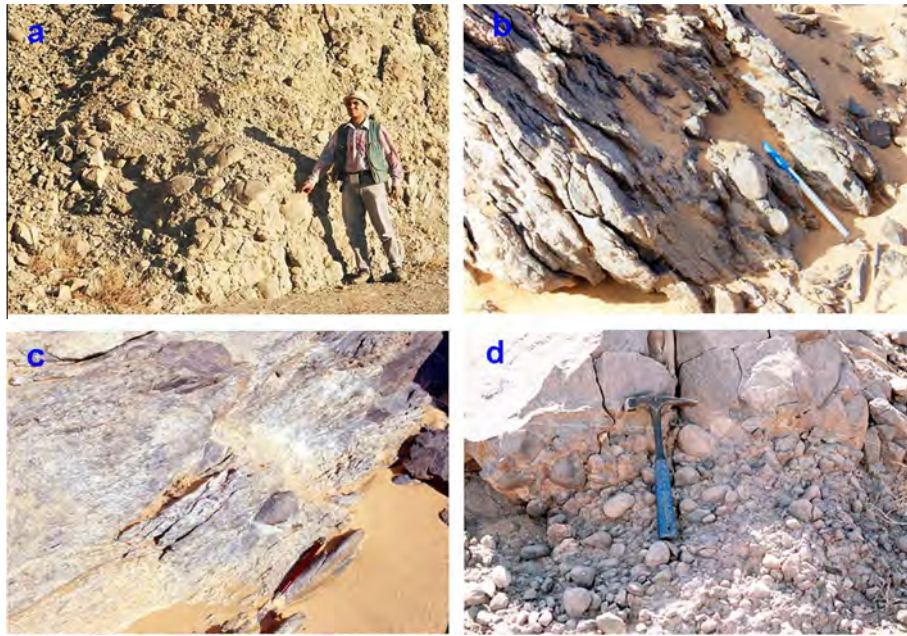


Fig. 12. Field photographs of the Hammamat polymictic conglomerates: (a) Field photograph of the Umm Gheig conglomeratic bed showing boulders, cobbles and pebble-size fragments. (b and c) Field photographs of the Allaqi conglomeratic beds. (d) Field photograph of Wadi Hodein conglomeratic layer underlying acidic volcanics.

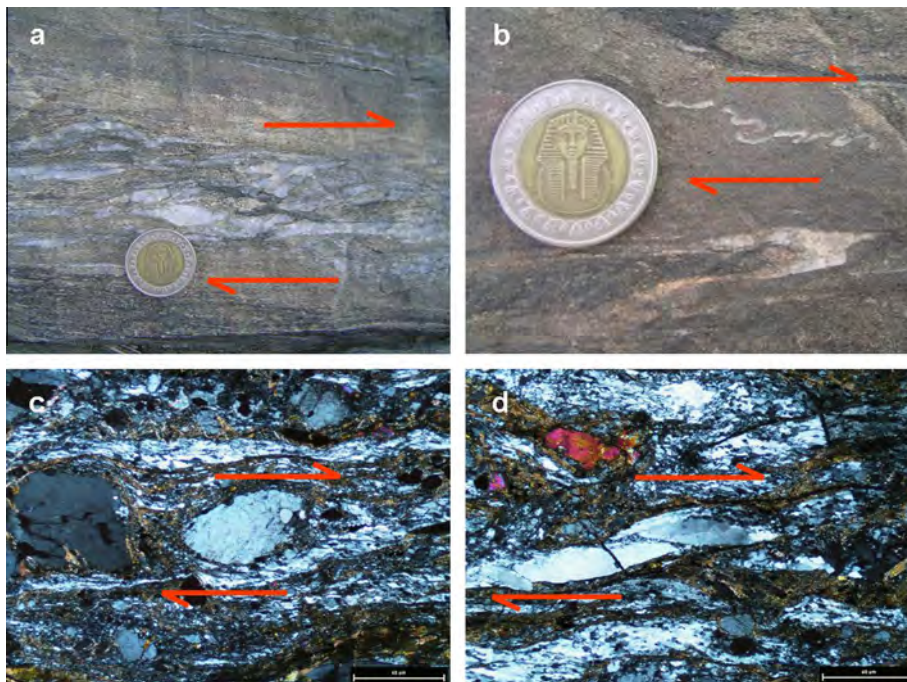


Fig. 13. Kinematic indicators reflecting dextral shearing along Wadi Fatima Shear Zone. (a and b) Close up view showing sigmoidal shapes of quartz ribbons and overturned Mesoscopic folding within amphibolite. (c and d) Microphotographs showing porphyroclasts of quartz with monoclinic symmetry, rotated in a dextral sense.

under the microscope in the intensively mylonitized granite (Fig 13). Such shearing is concordant with that recorded in the NE-oriented mega shears in the Arabian Shield, such as the Ad-Damm Shear Zone (Matsah et al., 2004; Hamimi et al., 2014). The Wadi Fatima and Ad-Damm Shear Zones are dextral and trending NE perpendicular to the NW-trending Najd Faults. Therefore, it is believed to be conjugate shears for the Najd Shear System (Davies, 1984). Recognition of dismembered ophiolitic slabs in

the vicinity of Wadi Fatima led Hamimi et al. (2013) to consider such conspicuous structure in the western Arabian Shield as an arc–arc suture; Wadi Fatima Suture Zone. Deposition of the volcanosedimentary succession within the FPADB was influenced somehow with dextral shearing along WFSZ, where the Fatima Group was deposited in a NE-oriented basin, and was folded and down faulted along WFSZ. In the Fatima Group, well-developed folds and thrusts at different scales are observed, referring that both

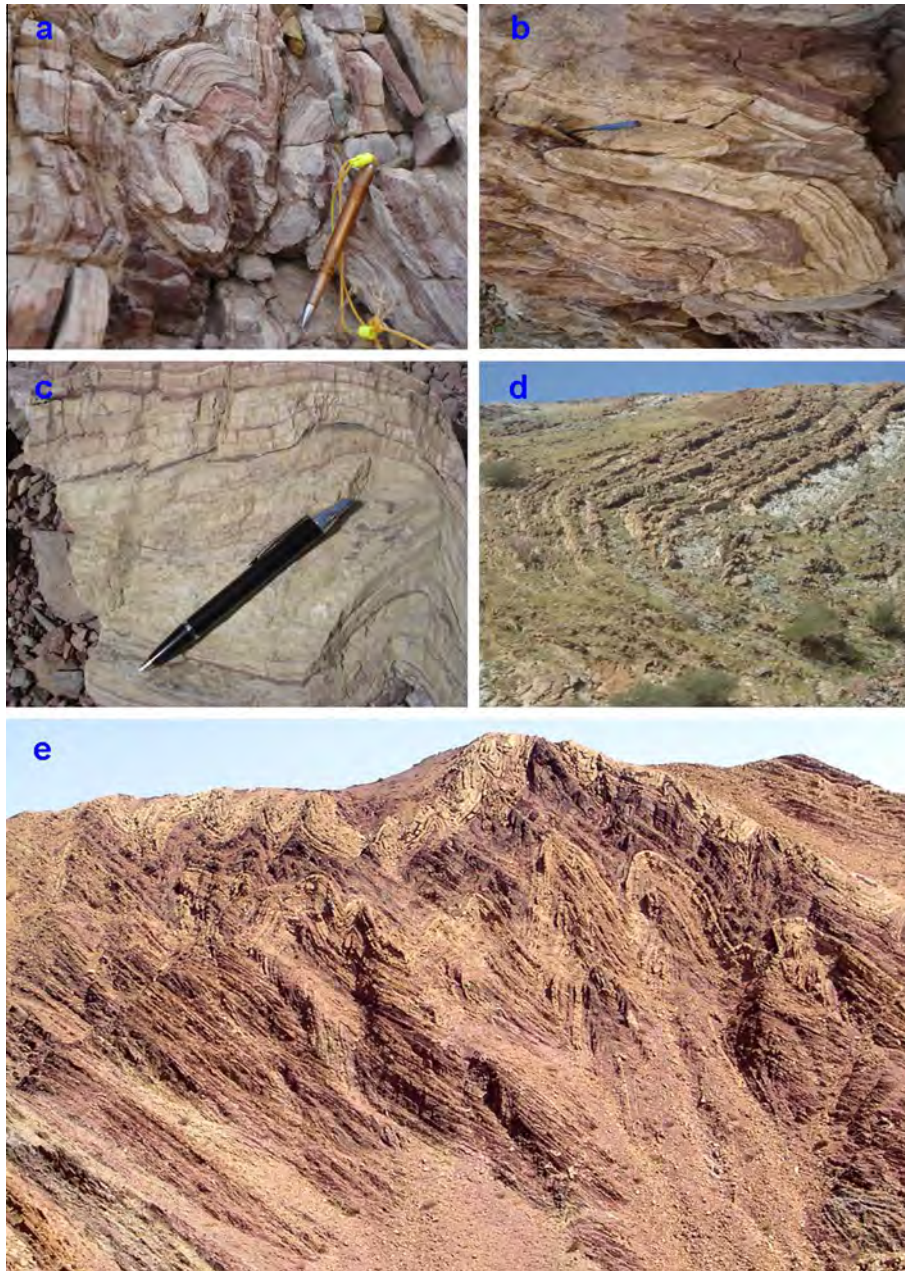


Fig. 14. Field photographs showing the deformation pattern in the FPADB. (a) F_1 tight folds in Daf Formation exhibiting variable orientations throughout the FPADB due to the effect of later deformation. (b and c) Thrusting and thrust-related folding in the middle Shubayrim Formation of the Fatima Group. (d and e) Well-developed F_2 thrust-related folding in Shubayrim Formation.

folding and thrusting are geometrically- and kinematically-related (Figs. 14 and 15) (Al-Gabali, 2012; Alsubhi, 2012). Several lines of field evidence confirm fold-first kinematics (i.e. thrusting was initiated as a consequence of folding) in the Fatima Group volcano-sedimentary sequence. Among these evidence are: (1) the geometry of interacting outcrop- and map-scale folds and thrusts, (2) patterns of thrust displacement variations and (3) indications for hinge migration during fold growth. Overprinting and superposed relations detected in the field indicate that the Fatima Group itself has undergone a deformation history involving at least three phases of deformation. Three main deformation events (D_1 , D_2 and D_3) constrained the Fatima Group. It is worthily to mention that these D_1 – D_3 deformation events are not documented in fabrics of pre- D_1 dextral shear deformation although the Fatima Group is

autochthonous and deformed in situ. D_1 is manifested by tight isoclinal F_1 folds, with variable orientations. D_2 is represented by F_2 thrust-related folds that are regularly overturned and/or inclined, with mild southeastern limbs and steep northwestern overturned limbs. The direction of overturning (folding vergence) varies from NW to NNW, and occasionally to N. In profile, the F_2 geometry is concentric and ranging from angular to curvilinear, and their axes are gently plunging NE to ENE. Because of large differential flow associated with thrusting, some parts of the fold axial regions may advance relative to other parts, forming sheath or eye folds. In such case, the fold axes become folded and the folded layers look like the finger of a glove or the sheath of a knife. D_3 is marked with F_3 open folds that are moderately to steeply plunging towards the SE to SSE direction. The collected field measurements from bedding

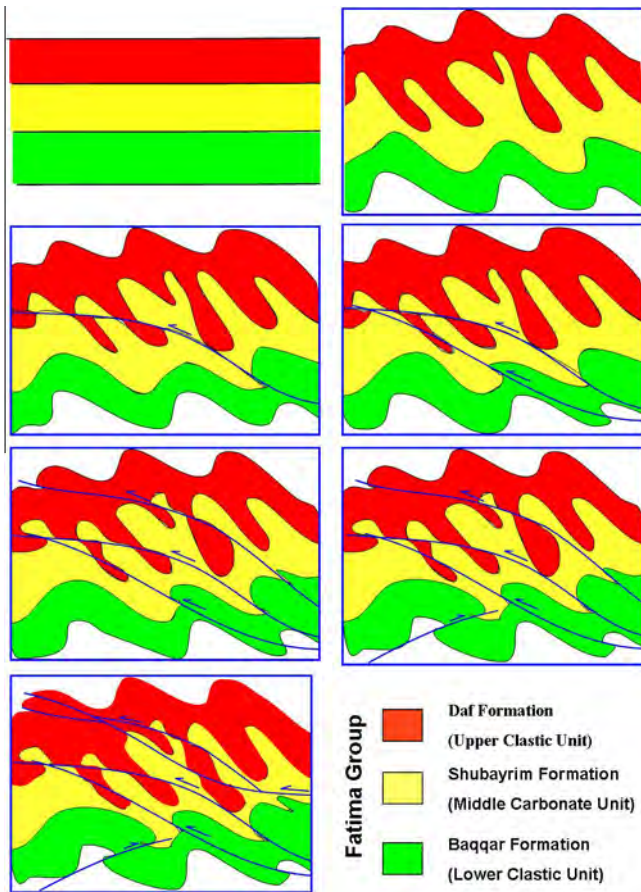


Fig. 15. Sketches showing the relation of folding to thrusting, and how thrusts were initiated and propagated in Fatima Group.

planes, fold hinges and oriented deformed pebbles are plotted and contoured using “Spheristat v. 2.2” Software Program (Fig. 16). The bedding planes are generally striking NE–SW and dipping toward NW and SE (Fig. 16a). F_1 fold hinges show variable orientations in the field because of the effect of the later deformation, and the number of the measured hinges is insufficient to be plotted on the Stereonet. The poles to the bedding exhibit a girdle distribution, $323^\circ/80^\circ$ SW (Fig. 16b), revealing folding about an axis plunging 10° toward the $N52^\circ$ E, coaxial to the F_2 folding axis (Fig. 16c and d) which is plunging 8° towards $N 81^\circ$ E. The F_3 folding axis is plunging 26° toward $S31^\circ$ E. The plots of the oriented deformed pebbles (Fig. 16e and f) are matched with the F_2 plots, plunging 12° towards the $N79^\circ$ E.

3.2. Deformation pattern in Ablah Basin

Composite folding, thrusting and shearing are complex structural fabrics characterizing the Ablah Group exposed either in its type locality near Jabal Ablah or in Wadi Yiba in Asir tectonic terrane. Superimpositions of these structural fabrics differentiated three main deformation events (D_1 , D_2 and D_3) (Fig. 17). D_1 documents an early bulk E–W (to ENE–WSW) shortening that resulted in East and West Gondwana suturing (Hamimi et al., 2012a). Structures designated as D_1 include mesoscopic folds (F_1) and associated axial foliation (S_1) and mineral and stretching lineations (L_1), and boudinage structure. D_1 fabrics are not pervasive throughout the Ablah Group units where they frequently show different characteristics in different deformed lithologic

units. They comprise small-scale tight isoclinal and intrafolial folds (F_1). Sometimes, F_1 folds become overturned and are locally westward verging, and occasionally, only tightly appressed folds and sheared-out hinges are observed and the attitudes of F_1 folding axes show variable orientations due to overprinting of latter deformation. Original orientation of F_1 folds is un-restorable precisely because of subsequent complex D_2 and D_3 deformations. S_1 foliations mostly show a preferred orientation, although random and irregular S_1 foliations are dominant in the central part of the Wadi Yiba area due to reworking by the later deformations. S_1 foliations are oriented parallel to the original bedding S_0 . L_1 lineations are outlined by preferred orientation of syn-kinematic minerals. Most of L_1 mineral- and stretching-lineations show variable orientations most probably due to subsequent deformation events. The tectonic regime prevailed during the D_2 deformation phase affected Ablah Group exposed in Wadi Yiba was transpression which involves strike-slip shear accompanying with horizontal shortening and vertical lengthening in the shear plane (Sanderson and Marchini, 1984; Dewey, 1998). The sense of strike-slip shearing was dextral as indicated by the sigmoidal kinematic indicators with monoclinic symmetry (Fig. 18) that are encountered in many outcrops in Wadi Yiba, the dextral enechelon tension gashes of quartz veins in observed in the upper marble unit, and the mega-scale sigmoidal patterns recognized on Landsat images. During D_2 , N- to NNW-oriented thrusts are formed. Thrust propagation was responsible for the formation of F_2 thrust-related folds and infrequently thrust duplexes. F_2 thrust-related folds are frequently overturned, with gentle eastern limbs and steep western overturned limbs. Transcurrent shearing accompanied this phase was dextral as indicated by microscopic and mesoscopic shear sense indicators. It was responsible for the formation of F_2 shear zone-related folds. The F_3 fold hinges, L_3 crenulation lineation and kink bands are D_3 fabrics that pervasively overprint the earlier deformation structural features. The F_3 folds are eastward moderately to steeply plunging upright folds. The L_3 crenulation lineation and kink bands in the Ablah Group volcanosedimentary sequence deflect the S_2 foliation to dip in directions around the east. Figs. 19 and 20 show the stereoplots of the collected measurements of planar (bedding planes) and linear structures (fold hinges and oriented deformed pebbles) from Ablah Group volcanosedimentary sequence exposed at Wadi Yiba area. The bedding planes strike NNW–SSE and dipping towards NE (Fig. 19a). As in Fatima Group, the poles to the bedding show a girdle distribution (Fig. 19b), $334^\circ/17^\circ$ SW, indicating folding about an axis plunging 73° toward the $N63^\circ$ E. F_1 fold hinges form two concentrations, plunging 28° and 14° toward $N22^\circ$ E and $N8^\circ$ W, respectively (Fig. 19c and d). F_2 fold hinges gave one concentration plunging 19° towards $N2^\circ$ E (Fig. 19e and f). F_3 fold hinges expose one concentration plunging 39° towards $N69^\circ$ E (Fig. 20a and b). The plots of the oriented deformed pebbles (Fig. 20c and d) coincide with the F_2 fold hinges, plunging 37° nearly towards $N4^\circ$ E.

3.3. Deformation pattern in Hammamat-type basins

The fault-bounded Hammamat basins are formed during late Pan-African NW–SE trending orogen-parallel crustal extension in the ANS (Fritz et al., 1996; Fritz and Messner, 1999; Abdeen and Greiling, 2005). The Hammamat sediments are autochthonous and nonconformably overly the basement rocks (Abdeen et al., 1992; Rice et al., 1993). They are intruded by late orogenic granites, dated with ca. 590 Ma (Rice et al., 1993). The NW-verging folds and SE-dipping thrusts (Greiling et al., 1994; Abdeen and Greiling, 2005) imply NW–SE oriented (D_1) compression (Fig. 21). This phase of NW–SE shortening was followed by a transpressional wrenching phase (D_2) related to the Najd Shear System, which

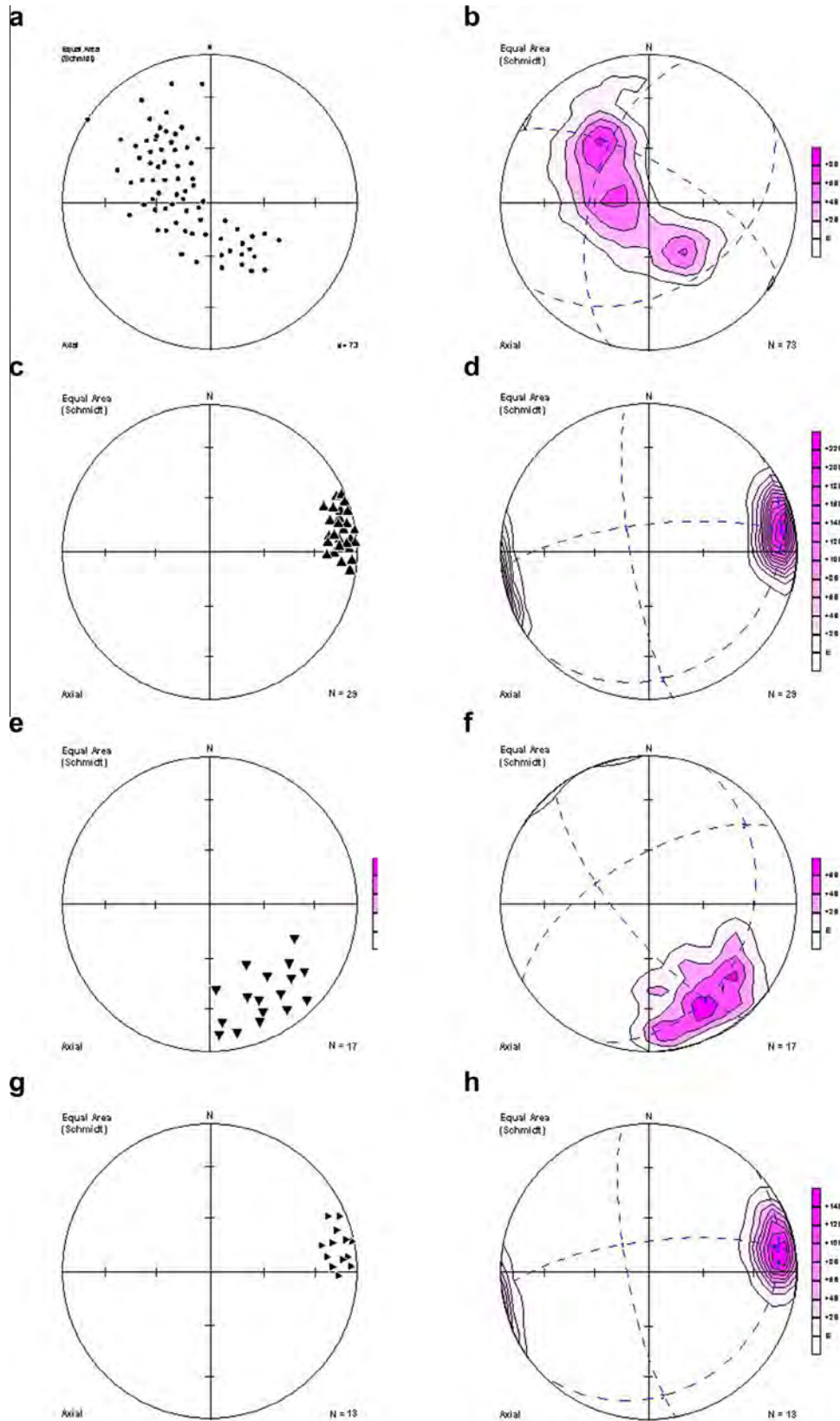


Fig. 16. Stereonet projections (equal area projection, lower hemisphere) showing (a and b) pole diagram and its contour equivalents of 73 bedding planes measured from Fatima Group outcrops. (c and d) Point and contour diagrams of 29 small F₂ fold hinges. (e and f) Point and contour diagrams of 17 small F₃ fold hinges. (g and h) Point and contour diagrams of 13 oriented deformed pebbles.



Fig. 17. Field photographs showing the deformation pattern in the APADB. (a) F_1 very tight isoclinal folds in the lower metaclastic unit. (b) F_1 nearly upright mesoscopic fold in the lower metaclastic unit. (c) F_2 thrust-related folds in the upper metaclastic unit. (d) F_2/F_1 superposition in the upper marble unit. (e) F_1 tight fold superposed by F_3 open fold in the upper metaclastic unit.

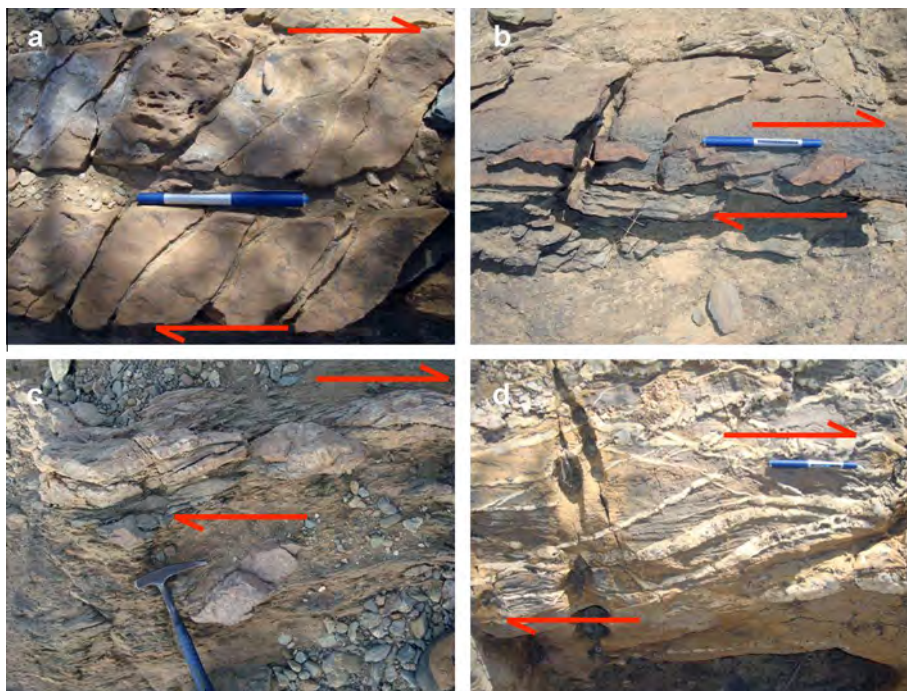


Fig. 18. Kinematic indicators revealing dextral shearing along Wadi Yiba Shear Zone. (a and b) Duplexing and imbrication of a single marble layer. (c and d) Sigmoidal quartz veins.

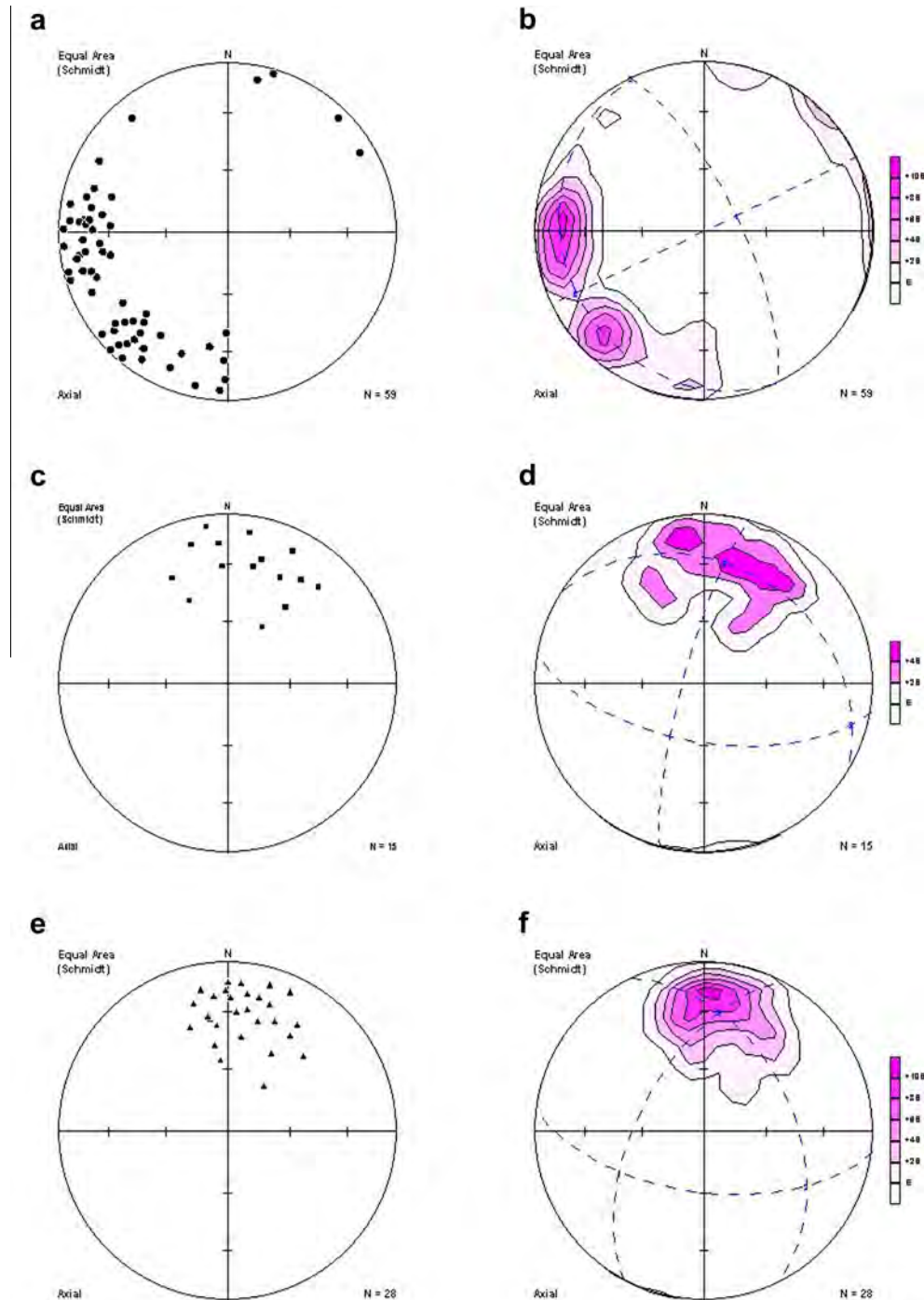


Fig. 19. Stereonet projections (equal area projection, lower hemisphere) showing (a and b) pole diagram and its contour equivalents of 59 bedding planes measured from Ablah Group outcrops exposed at Wadi Yiba area. (c and d) Point and contour diagrams of 15 small F₁ fold hinges. (e and f) Point and contour diagrams of 28 small F₂ fold hinges.

produced NW–SE sinistral faults associated with positive flower structures comprising NE-verging folds and SW-dipping thrusts (Abdeen, 2003; Abdeen et al., 1992; Abdeen and Greiling, 2005). At a regional scale, the two post-Hammamat shortening phases (NW–SE shortening associated with D₁ and NE–SW shortening associated with D₂) yielded an interference pattern with domes and basins. Stereographic projection of longest axis of stretched conglomeratic pebbles of the three studied Hammamat-related sedimentary basins (Fig. 22) shows preferred orientation towards NNW–SSE.

4. Strain analyses

4.1. Methods

Several methods have been applied in the determination of finite strain in naturally deformed rocks from deformed aggregates. In the present study, we calculated two-dimensional finite strain for each of the studied PADBs; Fatima, Ablah and Hammamat PADBs, using the most widely employed and popular Rf/ϕ method. This method which was first described by (Ramsay, 1967) is based on

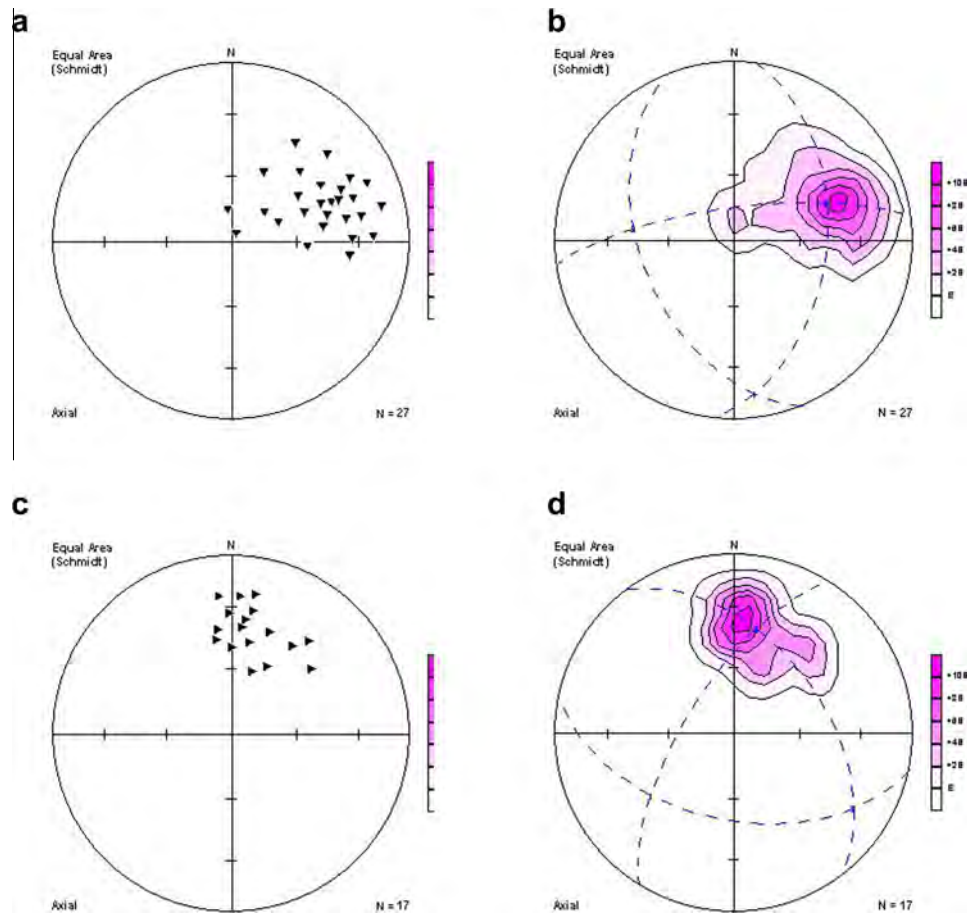


Fig. 20. Stereonet projections (equal area projection, lower hemisphere) showing (a and b) point and contour diagrams of 27 small F₃ fold hinges. (c and d) point and contour diagrams of 17 oriented deformed pebbles, collected from Ablah Group outcrops exposed at Wadi Yiba area.

the centre-to-centre distances between “nearest neighbors” components of the deformed material plotted against the orientations of the individual tie lines with reference to a chosen direction (Roday et al., 2010). As it is too time-consuming and laborious for practical construction, it has been enhanced and refined over the years by some authors (e.g. Dunnet, 1969; Lisle, 1985). Recently, several computer software have precisely tackled the Rf/φ method in finite strain calculations (e.g. Mulchrone and Meere, 2001; Chew, 2003; Wallbrecher, 2012). The Rf/φ technique has been

successfully applied to many geological situations and can potentially be used on any deformed suite of initially elliptical strain markers (e.g. conglomerates, oolites, etc.). The axial ratios (Rf) of typically between 50 and 100 strain markers and their respective long axes orientations (φ) have to be recorded. In the present work, Chew's (2003) spreadsheet (CSS) for finite strain analysis using the Rf/φ technique is used. The CSS comprises four worksheets and the first one is used to enter the data. In order to extract data relevant to strain analysis (long and short axes of the deformed pebbles; a , b , and the angle between the long axis and the reference line; φ) to use CSS, we used the Semi-Automatic Parameter Extraction program (SAPE) written by Mulchrone et al. (2005). The SAPE rapidly extracts the required strain parameters by means of a simple region-growing algorithm to identify regions of interest from input digital images saved in bitmap format. The input images needed to use the SAPE are manually produced by tracing the outlines of the deformed polymictic conglomeratic pebbles encountered in the studied PADB's using CorelDRAW. Tracing of the outlines were carried out on images taken from outcrops, as well as those taken from polished surface samples and oriented thin sections. The samples were cut parallel to the lineation (mineral elongation) and fold axes, and perpendicular to the foliation. The Rf and φ parameters extracted using the SAPE have also been the subject matter of finite strain estimation using the Mean Radial Length (MRL) of Mulchrone et al. (2003). The MRL calculates finite sectional strain from distributions of elliptical objects. The only assumptions required to apply this software are that before deformation (1) long axis orientations are uniformly distributed, (2) the

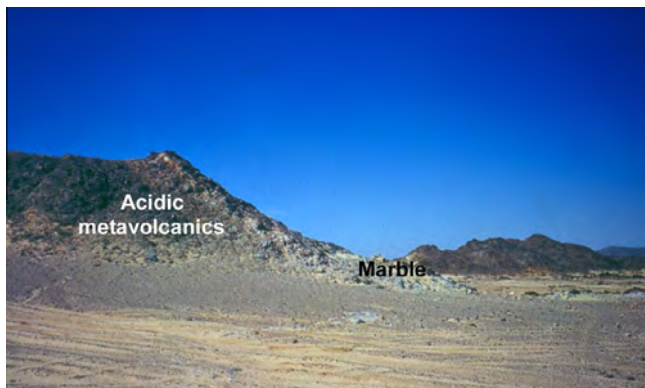


Fig. 21. Field photograph of a thrust sheet of marble and associated conglomeratic layers as part of post amalgamation shelf sediments overlying acidic metavolcanics in the central part of Wadi Allaqi, looking NW.

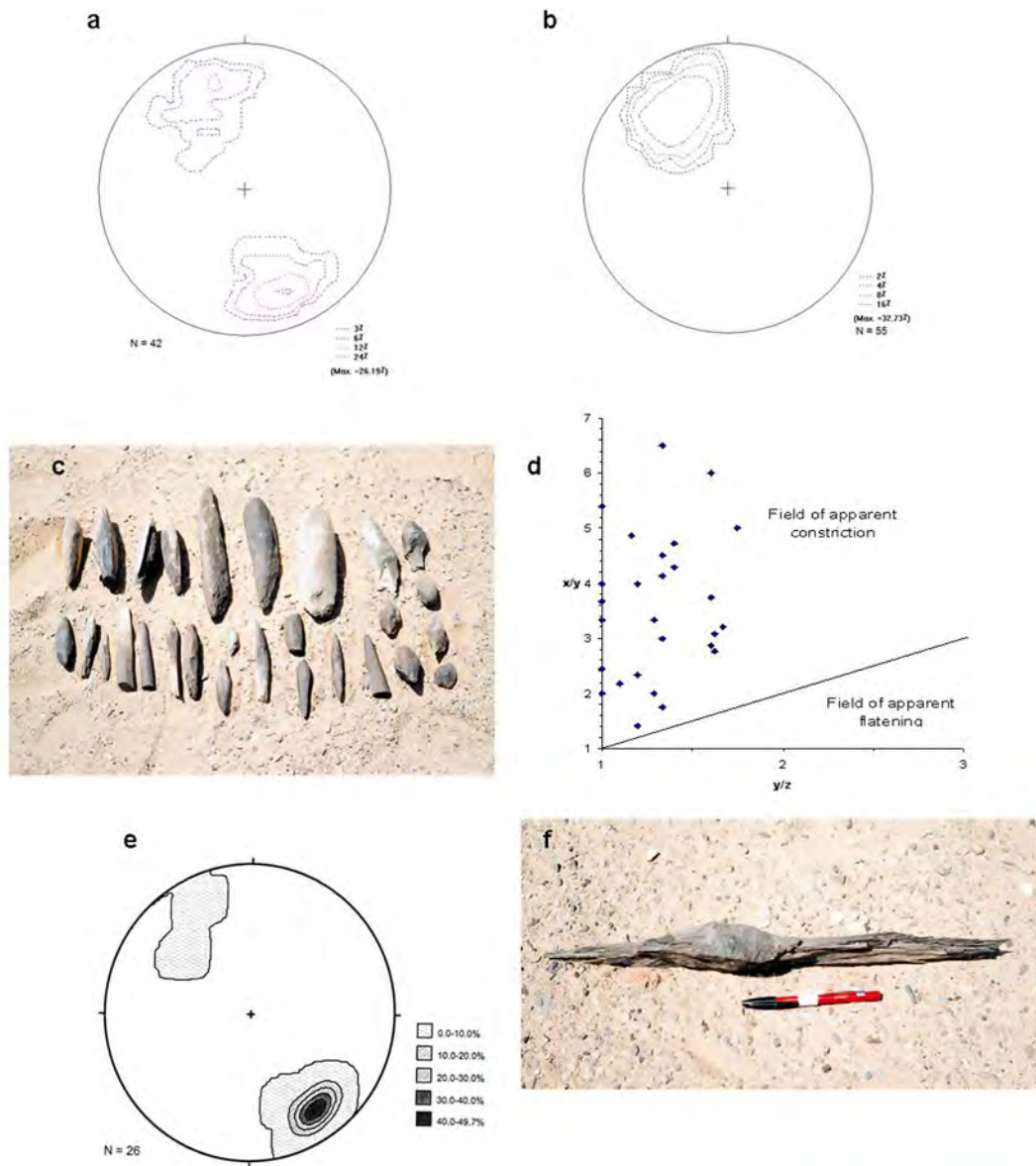


Fig. 22. Stereonet projections (equal area projection, lower hemisphere) of longest axis of stretched conglomeratic pebbles of the three studied Hammamat-related sedimentary basins showing NNW–SSE preferred orientation. (a) Umm Gheig, (b) Allaqi, and (c–f) Wadi Hodein.

distribution of axial ratios is independent of orientation, (3) homogenous deformation and (4) no ductility contrast between strain markers and their matrix. The method is based on the conceptually simple fact that the mean radial length of a set of uniformly oriented ellipses in the unstrained state equates to that of a circle, so that after strain, the mean radial length evaluates to the strain ellipse.

4.2. Results

The outputs of average strain calculations of deformed polymictic conglomerates in selected Fatima, Ablah and Hammamat PADBs are tabulated in Table 1 and graphically presented in Figs. 23–30. The inspection of the results of the CSS and MRL implies that strain parameters of the three PADBs are closely compatible and consistent. Table 2 shows the Vector mean, the Harmonic mean, the Ln Harmonic mean and the I_{SYM} obtained from the CSS. The ANOVA test carried out on the Vector mean, the Harmonic mean, the Ln Harmonic mean and the I_{SYM} obtained from the CSS (Table 3) indi-

cates no significant difference for the Vector mean and I_{SYM} for the investigated PADBs. There is only a significant difference for the Harmonic mean (P -value < 0.05). A Post Hoc test (Shefee) shows that the difference exists between the Allaqi and the Umm Gheig's deformed polymictic conglomeratic pebbles of the Hammamat Post-amalgamation Depositional Basin (HPADB) (Fig. 31).

5. Discussion

5.1. Depositional events in the Arabian–Nubian Shield

The ANS lies at the northern part of the East African Orogen (EAO; Stern, 1994) and represents the upper crustal equivalent of the high-grade Mozambique Belt. The juxtaposition of the ANS low-grade basement rocks and the high-grade rocks of the Mozambique Belt is documented in many areas, such as in southern Ethiopia (Yihunie and Tesfaye, 2002), particularly in the vicinity of the SE-dipping, top-to-the-SE, low-angle shear zone that developed during regional gravitational tectonic collapse (Tsige

Table 1
Average of MRL strain data for the investigated deformed polymictic conglomerates in the three PADBs.

Method	Rs (Lower)	Rs	Rs (upper)	φ (lower)	φ	φ (upper)
<i>A: Average of MRL strain data for the deformed polymictic conglomerates of Fatima area</i>						
Mulchrone et al. (2002)	1.26	1.36	1.52	–28.66	–8.63	–4.71
	1.26	1.37	1.52	–23.64	–11.97	7.97
	1.27	1.37	1.47	–23.64	–11.97	–1.33
Mulchrone and Meere (2001)	1.17	1.38	1.85	–23.52	–11.97	–1.30
Yu and Zheng (1984)	1.22	1.40	2.01	–23.75	–11.97	–1.52
Harmonic mean	1.70	1.83	1.99	N//A	N//A	N//A
Geometric mean	1.78	1.93	2.06	N//A	N//A	N//A
Arithmetic mean	1.87	2.04	2.21	N//A	N//A	N//A
Mulchrone (2004)	1.20	1.36	1.50	–26.11	–8.63	8.85
<i>B: Average of MRL strain data for the deformed polymictic conglomerates of Yiba area</i>						
Mulchrone et al. (2002)	1.56	1.75	1.96	–1.68	2.98	8.47
	1.54	1.73	1.98	87.92	93.23	99.20
	1.61	1.73	1.85	87.92	93.23	99.20
Mulchrone and Meere (2001)	1.28	1.67	2.26	87.82	93.23	99.30
Yu and Zheng (1984)	1.76	2.39	3.87	–2.09	3.23	9.57
Harmonic mean	1.72	1.89	2.14	N//A	N//A	N//A
Geometric mean	1.82	2.01	2.28	N//A	N//A	N//A
Arithmetic mean	1.92	2.16	2.44	N//A	N//A	N//A
Mulchrone (2004)	1.32	1.75	2.27	–2.46	2.98	8.42
<i>C: Average of MRL strain data for the deformed polymictic conglomerates of Um Gheig area</i>						
Mulchrone et al. (2002)	1.29	1.42	1.57	–13.30	8.493	18.32
	1.28	1.42	1.56	–13.12	8.63	19.23
	1.32	1.42	1.52	–13.12	8.63	19.23
Mulchrone and Meere (2001)	1.12	1.39	1.74	–13.25	8.63	19.23
Yu and Zheng (1984)	1.26	1.56	2.09	–13.33	8.63	19.66
Harmonic mean	1.56	1.69	1.81	N//A	N//A	N//A
Geometric mean	1.62	1.75	1.89	N//A	N//A	N//A
Arithmetic mean	1.69	1.84	1.99	N//A	N//A	N//A
Mulchrone (2004)	1.27	1.42	1.57	–14.23	8.49	18.06
<i>D: Average of MRL strain data for the deformed polymictic conglomerates of Allaqi area</i>						
Mulchrone et al. (2002)	2.04	2.32	2.66	29.25	33.90	38.10
	2.06	2.39	2.71	27.72	33.31	38.22
	2.26	2.39	2.51	27.72	33.31	38.22
Mulchrone and Meere (2001)	1.22	2.47	3.10	27.80	33.31	38.33
Yu and Zheng (1984)	1.99	2.46	4.09	28.09	33.31	38.30
Harmonic mean	2.39	2.69	3.03	N//A	N//A	N//A
Geometric mean	2.59	2.91	3.25	N//A	N//A	N//A
Arithmetic mean	2.79	3.13	3.45	N//A	N//A	N//A
Mulchrone (2004)	1.98	2.32	2.67	29.54	33.90	38.26
<i>E: Average of MRL strain data for the deformed polymictic conglomerates of Hodein area</i>						
Mulchrone et al. (2002)	1.33	1.43	1.54	36.88	43.65	50.55
	1.33	1.43	1.54	34.85	41.93	49.51
	1.35	1.43	1.50	34.85	41.93	49.51
Mulchrone and Meere (2001)	1.20	1.47	1.80	34.79	41.93	49.42
Yu and Zheng (1984)	1.29	1.52	1.84	34.52	41.93	49.38
Harmonic mean	1.62	1.71	1.82	N//A	N//A	N//A
Geometric mean	1.67	1.77	1.88	N//A	N//A	N//A
Arithmetic mean	1.72	1.83	1.96	N//A	N//A	N//A
Mulchrone (2004)	1.32	1.43	1.54	36.88	43.65	50.42

and Abdelsalam, 2005). The Neoproterozoic juvenile arc terranes of the ANS involves a collage of polydeformed and variably metamorphosed arc-related volcanosedimentary associations that are intruded by voluminous granitoids and gabbroic intrusions with enclaves of pre-Neoproterozoic crust (Johnson et al., 2011). The ANS involves two main depositional events over its long-time of deformation history; (1) the early depositional event, predated 650 Ma, is characterized by an arc- and back arc-related volcanosedimentary associations; and (2) the late depositional event, postdated 650 Ma, is dominated by PADBs-related volcanosedimentary sequences overlying the newly amalgamated arc terranes (Johnson et al., 2011). The development of the PADBs is regarded as an expression of the tectonic heterogeneity that involving diachronous deformational and crust-forming events. It was prevailed in the 150–100 Ma span (between the 680–640 Ma amalgamation event) in the eastern Arabian Shield and accompanied the transformation of the entire northern EAO into a passive

margin on the southern flank of palaeo-Tethys (Johnson, 2003). Furthermore, the abundance of the PADBs, and the presence of marine deposits in some, implies that large areas of the ANS were depressed during the late Cryogenian and Ediacaran so as to accommodate thick sequences of sedimentary and volcanic rocks and significant parts were below sea level (Johnson et al., 2011). The foregoing suggestion raised some essential questions, such as, whether the EAO during its formation was a continuous or discontinuous, broken-up mountain belt, whether it was high above sea level and far from oceanic influences, or whether it was deeply penetrated by seaways along valleys and depressions.

5.2. The investigated depositional basins

The wealth of structural data gathered from the PADBs is not only important in understanding their own tectonic setting and evolution, but also significant in deciphering enigmatic issues

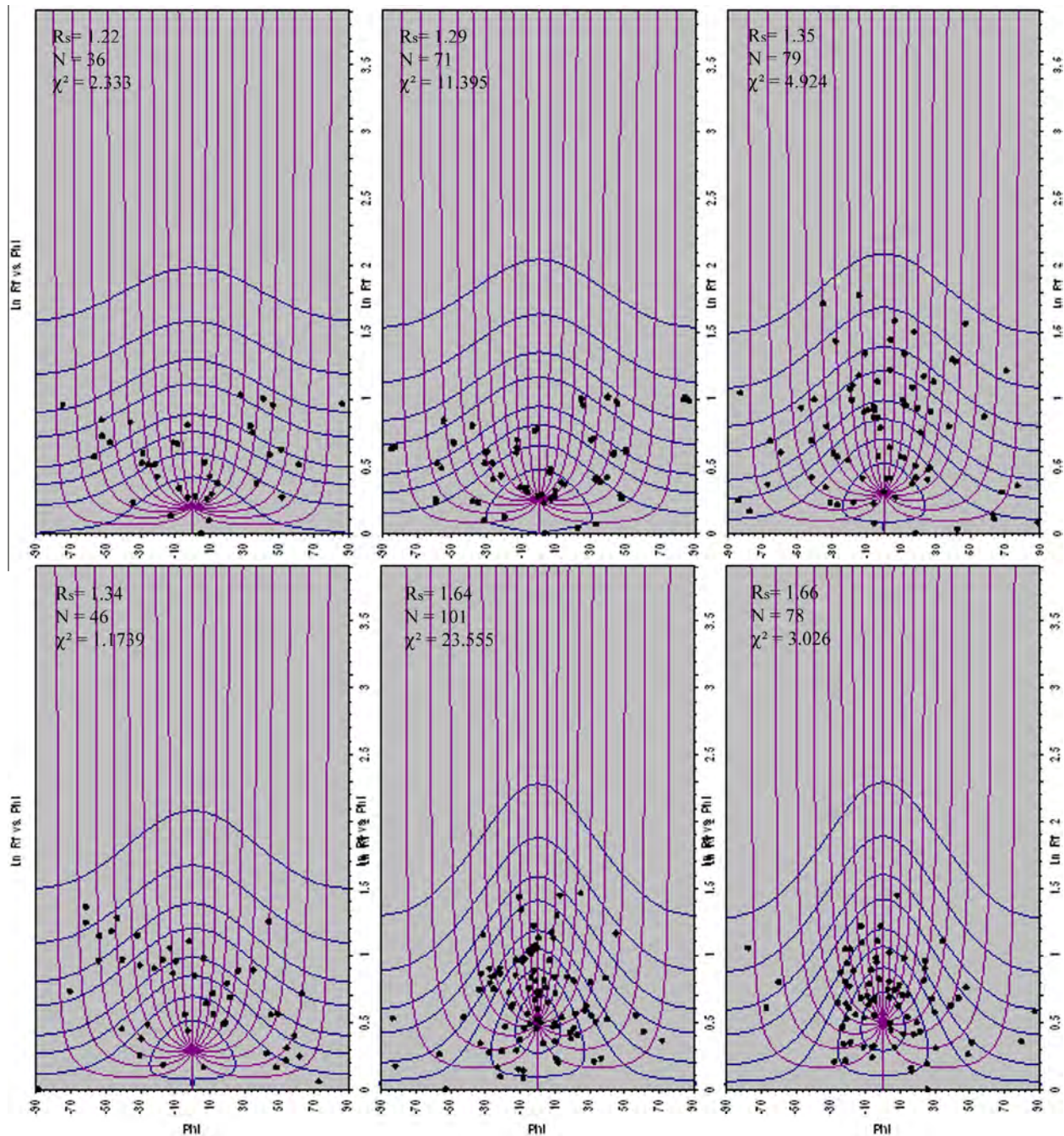


Fig. 23. Rf/ϕ plots (after Lisle, 1985) showing the strain ratios of the deformed pebbles of the Fatima Group.

and in unraveling questions that may emerge during the study of the ANS or even the whole EAO. It is useful also in interpreting the closing stages of Gondwana convergence and assembly. We have tried through the present work to highlight the much debatable deformation history of the PADBs in the ANS, based on detailed investigation of two PADBs in the Arabian Shield (Fatima and Ablah PADBs) and one basin in the Nubian Shield (Hammamat PADB). These three PADBs, together with the Murdama and the Jibalah PADBs, are the most famous throughout the entire ANS. The presence of an eye-catching carbonate unit (Shubayrim Formation), consisting of limestones, sandy limestones and marbles, with abundant crypogamminates and stromatolites, in the middle part of the Fatima Group indicates for the first glance that this group which was given a 688–680 Ma depositional age (Duyverman

et al., 1982; Darbyshire et al., 1983; Grainger, 2001) is definitely marine. It is worthy to mention here that Basahel et al. (1984) argue that the organic remains in the Fatima Group sedimentary sequence imply a Lower Cambrian age. The Ablah Group involves carbonate-rich units, which give a 614–610 Ma depositional age in Jabal Ablah type locality (Genna et al., 1999; Johnson et al., 2001). The PADBs carbonate-rich units in northeast of Asir terrane led Johnson (2003) to suggest that even if terrane assembly caused orogenic uplift, large parts of the northeastern Arabian Shield were subsided developing connections to the ocean flanking the emerging Gondwana supercontinent within a few million years of orogeny.

In contrast, the PADBs in Eastern Desert of Egypt contains about 4000 and 7500 m thicknesses of molasse-type sediments

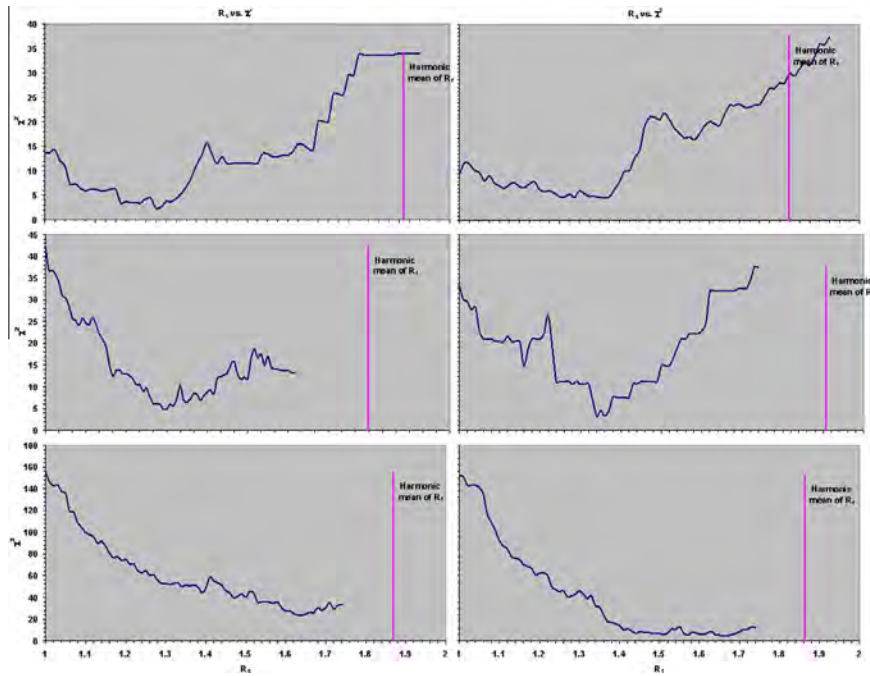


Fig. 24. Plotting of R_s vs. χ^2 illustrating how the best-fit parameters (χ^2) of θ -distribution text varies with strain (R_s) in the Fatima Group.

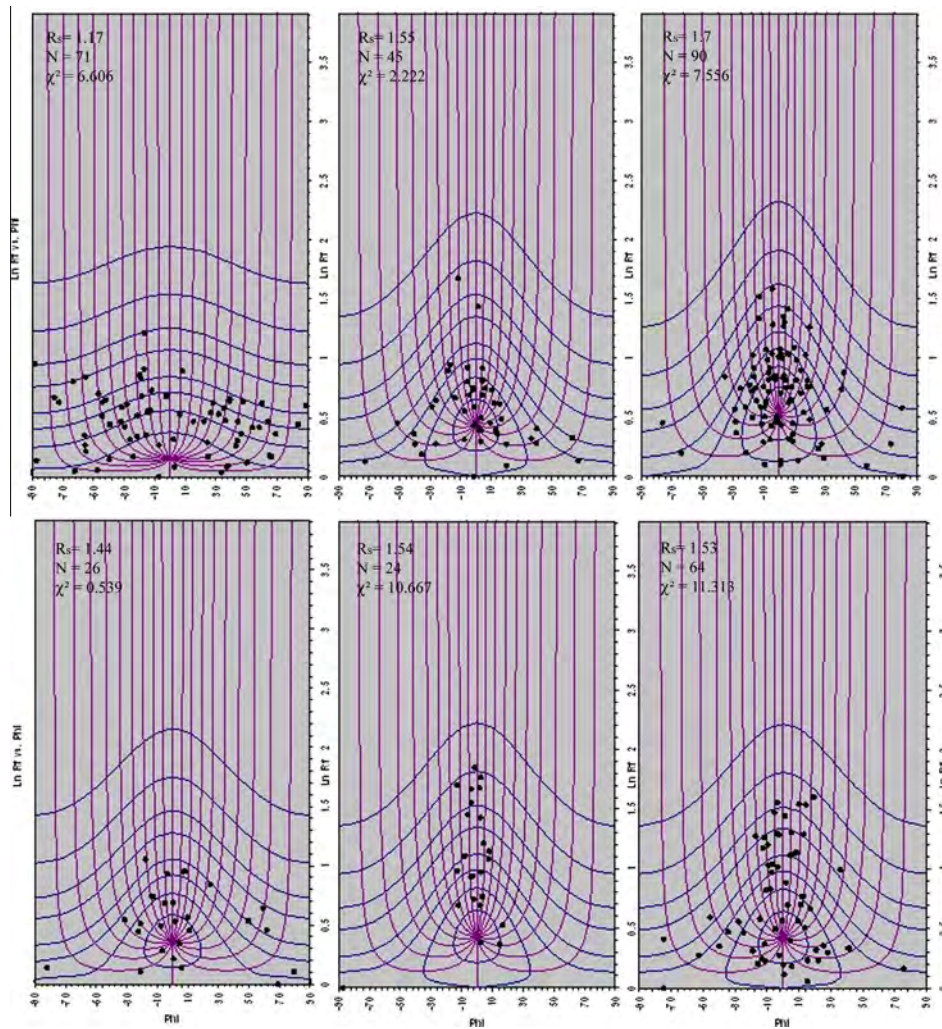


Fig. 25. R_f/ϕ plots (after Lisle, 1985) showing the strain ratios of the deformed pebbles of the Ablah Group exposed at Wadi Yiba.

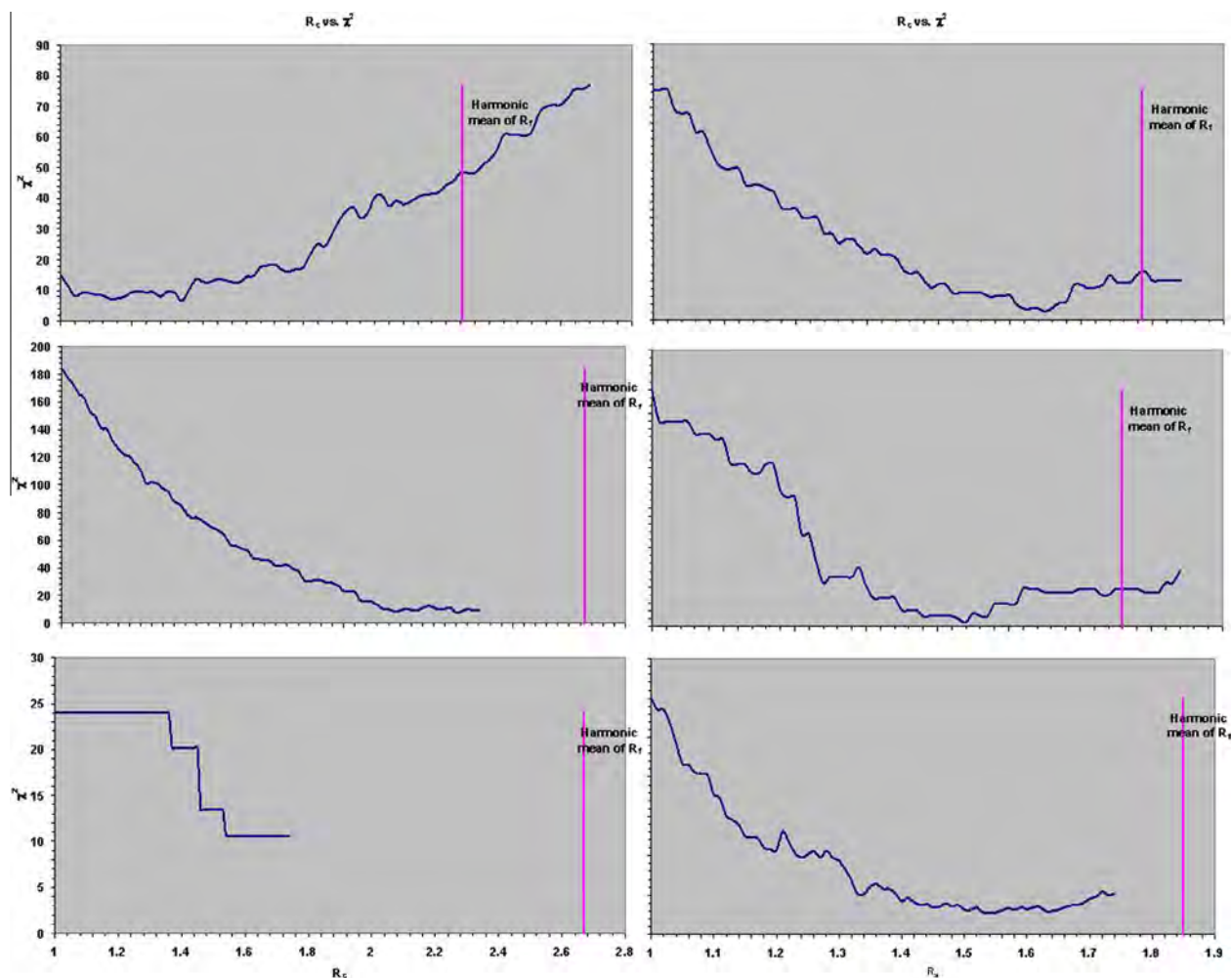


Fig. 26. Plotting of R_s vs. χ^2 illustrating how the best-fit parameters (χ^2) of θ -distribution text varies with strain (R_s) in the Ablah Group exposed at Wadi Yiba.

in Hammamat and Karim basins, respectively (Fritz and Messner, 1999; Abd El-Wahed, 2010). They account about 590 Ma depositional age containing intercalations of polymictic conglomerates, gritstone, sandstone, siltstone and claystone (Akaad and Noweir, 1969, 1980) of terrestrial derived sediments.

Nevertheless, the intimate relation of the Hammamat Group (590–585 Ma depositional age) to the Dokhan Volcanics is much debatable and questionable, as the sedimentary and volcanic rocks show variable distribution from PADB to another, and sometimes variable distribution is detected within the same Hammamat PADB. The Dokhan Volcanics typically include basaltic andesite, andesite, dacite, and rhyolite that some consider to be a bimodal suite (e.g. Stern and Gottfried, 1986; Mohamed et al., 2000) although this conclusion has been challenged by some authors (e.g. Eliwa et al., 2006) (Johnson et al., 2011). The variability in the sedimentary and volcanic distribution between the Hammamat and the Dokhan led authors to suggest four possible relations between the Hammamat Group and the Dokhan Volcanics; (1) the deposition of the Hammamat took place pre-dating volcanic activity of the Dokhan (e.g., Stern and Hedge, 1985; Willis et al., 1988), (2) volcanic activity of the Dokhan took place first, and the Hammamat in such case is younger than the Dokhan (e.g., Dardir and Abu Zeid, 1972; El Ramly, 1972; Akaad and Noweir, 1980; Ries et al., 1983; Hassan and Hashad, 1990), (3) both deposition of the Hammamat and volcanism of the Dokhan are contemporane-

ous (e.g. Ressetar and Monrad, 1983; Stern et al., 1984; Eliwa et al., 2010) and (4) the deposition of the basal part of the Hammamat is contemporaneous with the latest eruption of the Dokhan (rhyolites) (El-Gaby et al., 1989). Johnson et al. (2011) pointed out that the main problem in the Hammamat Group–Dokhan Volcanics interrelation is that both of them are defined based on facies. For this reason, Breitzkreuz et al. (2010) believed that the two facies should not be expected to occur in the same relative stratigraphic position in every PADB, simply because deposition took place in a dynamic setting around isolated volcanic centers and basin systems with different structural controls and different ages.

5.3. Lithological and tectonic similarity between Fatima and Ablah Basins

It is remarkably observed that the Fatima and Ablah Groups are lithologically comparable of marine origin. They occupy the PADBs west of Nabitah orogenic belt (680–640 Ma) that sutures the Afif and ANS terranes. Field-structural investigation reflects another matching from the tectonic point of view, where both groups were associated one way or another with strike-slip faulting and trans-current shearing, underwent a deformation history involving three phases of Neoproterozoic deformations and show geometric and kinematic relations between folding and thrusting. Additionally, the geometry of interacting outcrop- and map-scale folds and

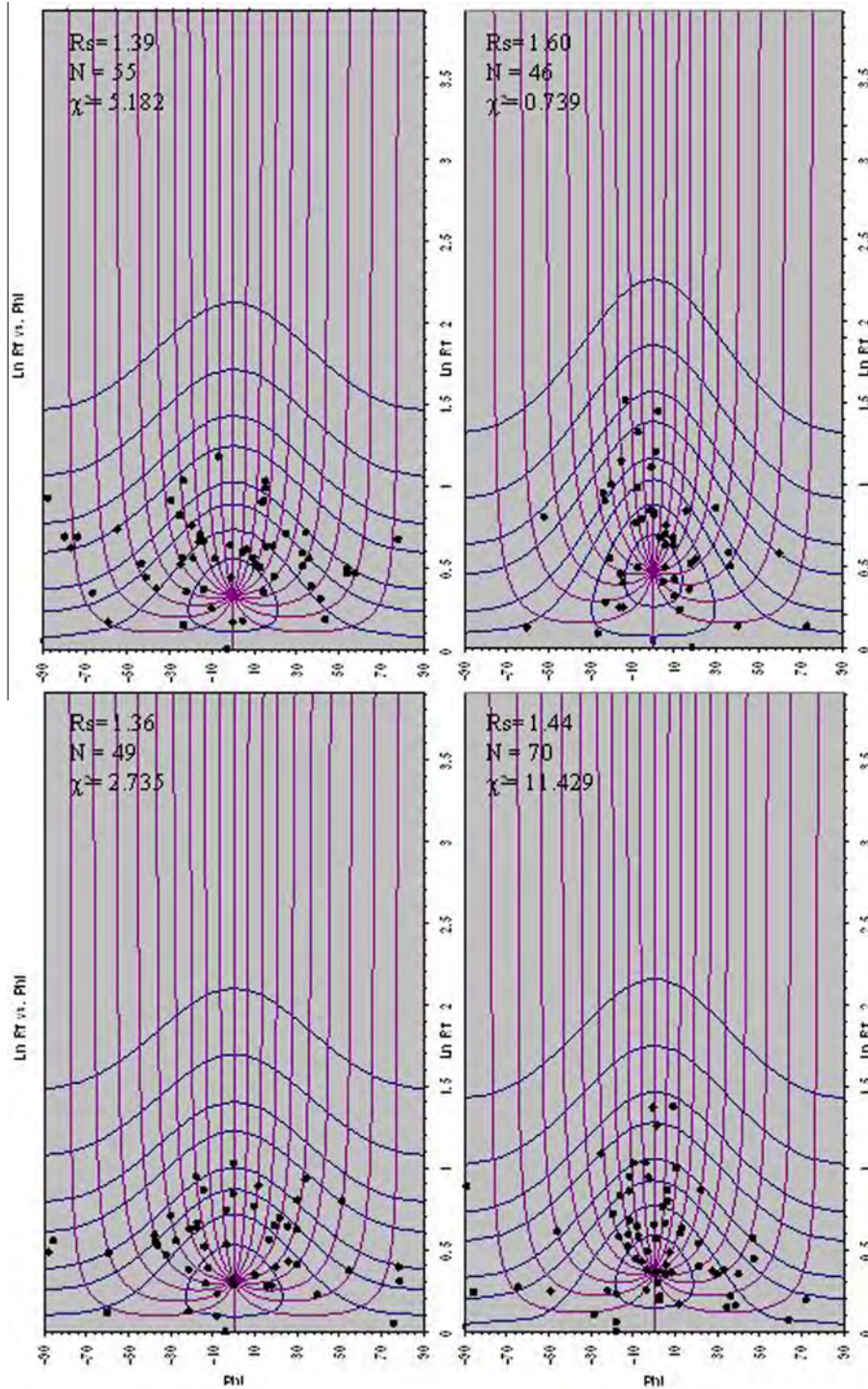


Fig. 27. Rf/ϕ plots (after Lisle, 1985) showing the strain ratios of the deformed pebbles of the Hammamat Group exposed at Wadi Umm Gheig.

thrusts, patterns of thrust displacement variations and indications for hinge migration during fold growth, strongly attest fold-first kinematics in both groups; i.e. thrusting was initiated as a consequence of folding in both groups. Thrusting and thrust-related folding were resulted from an intensive transpressional phase. The UFSZ transpressional shear zone involves a N–S right-lateral strike-slip shearing and an E–W bulk shortening. It deforms the boundary between the Ablah Group and Asir arc terrane at its central part (Moufti, 2001). Bulk E–W shortening was maintained during late phases of Gondwana assembly through convergence of East- and West Gondwanalands. Orientation of earlier fabrics are

disturbed by later deformations in the Fatima Group; however, they are slightly disturbed in the Ablah Group where bulk eastward plunging folds, kink bands and crenulation lineation commonly support a bulk N–S shortening. Miocene Red Sea rifting might contribute NE-tilting the Arabian Shield that perhaps disturb the basement fabrics.

5.4. Role of Najd Shear in structural shaping of the Hammamat Basin

In the Hammamat sediments, structures are clear and pervasive as those observed in the previously mentioned Fatima and Ablah

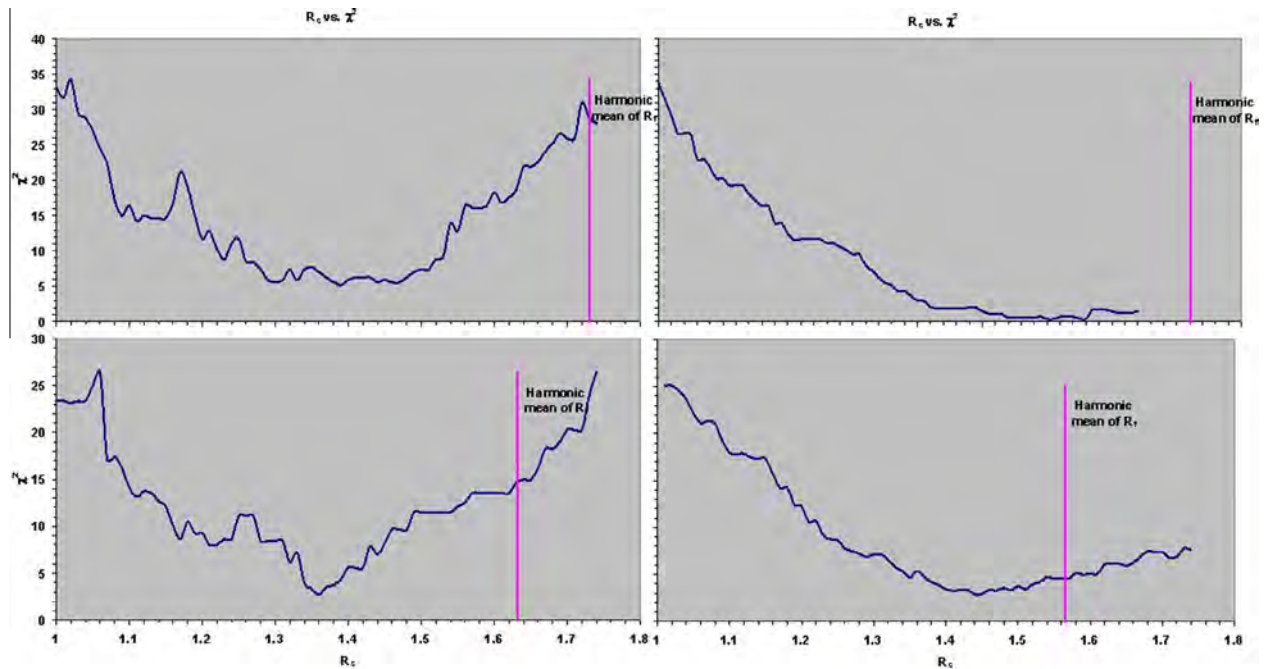


Fig. 28. Plotting of R_s vs. χ^2 illustrating how the best-fit parameters (χ^2) of θ -distribution text varies with strain (R_s) in the Hammamat Group exposed at Wadi Umm Gheig.

Groups. In this context, the wonderful structures encountered in both the Fatima and the Ablah Groups are nearly restricted to the carbonate units and to some extent in the andesitic sills and flows which are considered as marker horizons, particularly in the Jabal Abu Ghurrah-, Jabal Mukassar-, Jabal Daf- and Jabal Shubayrim – Fatima Group volcanosedimentary sequence. However, folding and thrusting in the HPADB seem also to be geometrically- and kinematically-related. The NW-verging folds on southward dipping thrusts (related to D_1) indicate that the HPADBs experienced a NW–SE oriented shortening post-deposition of molasse-type sediments. It is considered correlatable with the NW-trending shortening that affected the Fatima and Ablah PADBs. The overprinting of D_1 structures of the Hammamat PADB indicates that HPADBs were affected by a Najd Shear System-related transpressional wrenching (D_2), which played a significant role in the structural shaping and final geometry of the PADB, and resulted in the formation of NW–SE sinistral-slip faults, as well as positive flower structures comprising NE-verging folds and SW-dipping thrusts.

5.5. Comparison between the studied basins

Inspection of the foregoing discussion reveals a remarkable identity in tectonic regime prevailed in the Fatima and the Ablah Groups which deposited in marine environments in NE- and N-trending PADBs, respectively, in the Arabian segment of the ANS to the west of the axis of the Nabitah Mobile Belt. Both groups were associated with transcurrent shearing. The deformation patterns of PADBs in western Arabian Shield and Hammamat molasse sediments in Eastern Desert are alike. The only exception is the absence of the earlier-formed structures (D_1) that pre-dating the conspicuous transpressional phase (D_2) and formed due to the effect of an early E–W (to ENE–WSW) shortening phase accompanied with the convergence between East and West Gondwana. In particular, left-lateral strike-slip faults of Najd Fault System deform

the Hammamat in contrast to PADBs east of the Arabian Shield, which suggest that Hammamat sediments postdate the Fatima and Ablah PADBs. This conclusion is consistent with the 590–585 Ma depositional age of epiclastic Hammamat Group (Rice et al., 1993). The MRL and CSS strain calculations are consistent for all PADBs in the ANS, suggesting that they are correlated and underwent the same history of deformation. The results show no significant differences for the Vector mean and I_{SYM} . The only significant difference for the Harmonic mean (P -value < 0.05); a Post Hoc test (Shefee), is detected within the Hammamat Group volcanosedimentary sequence crops out in the Allaqi and Umm Gheig.

6. Conclusions

The results of our structural study and strain analyses of Fatima-, Ablah- and Hammamat-PADBs are summarized as follows:

- The Fatima PADB is controlled by dextral transcurrent shearing occurred along the NE-oriented Wadi Fatima Shear Zone in western Arabian Shield.
- The Ablah PADB is a strike-slip pull-apart basin in Asir tectonic terrane.
- The Hammamat PADB is a fault-bounded basin in the northern Nubian Shield.
- The Fatima and Ablah PADBs were affected by at least three Neoproterozoic deformation phases.
- Both basins show intimate geometric and kinematic relationships between folding and thrusting.
- The deformation patterns of PADBs in western Arabian Shield and Hammamat molasse sediments are alike.
- The MRL and CSS Strain calculations are consistent for the three investigated PADBs, suggesting that they are correlated and underwent the same history of deformation.

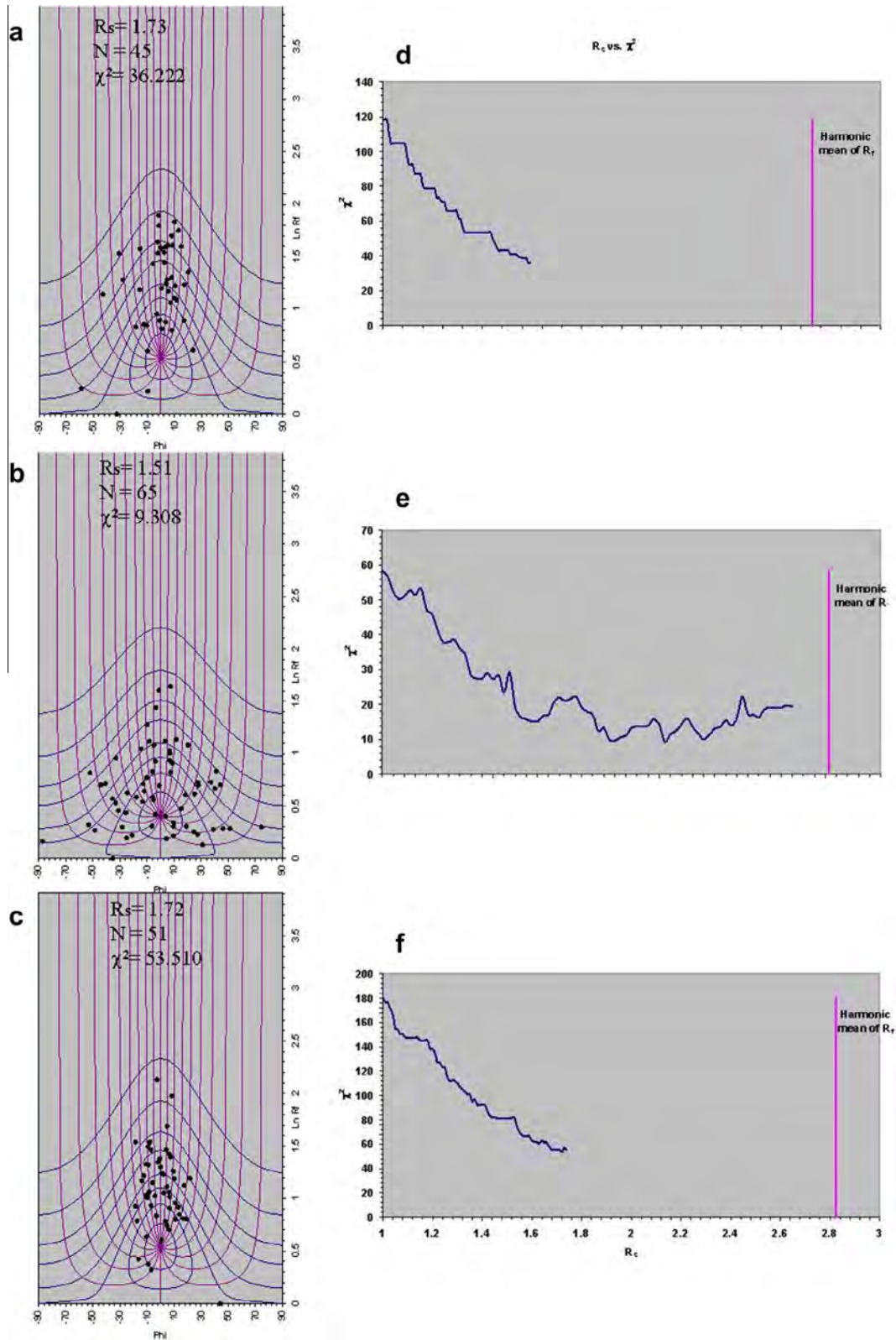


Fig. 29. (a–c) Rf/ϕ plots (after Lisle, 1985) showing the strain ratios of the deformed pebbles of the Hammamat Group exposed at Wadi Allaqi. (d–f) Plotting of R_s vs. χ^2 illustrating how the best-fit parameters (χ^2) of θ -distribution text varies with strain (R_s) in the Hammamat Group exposed at Wadi Allaqi.

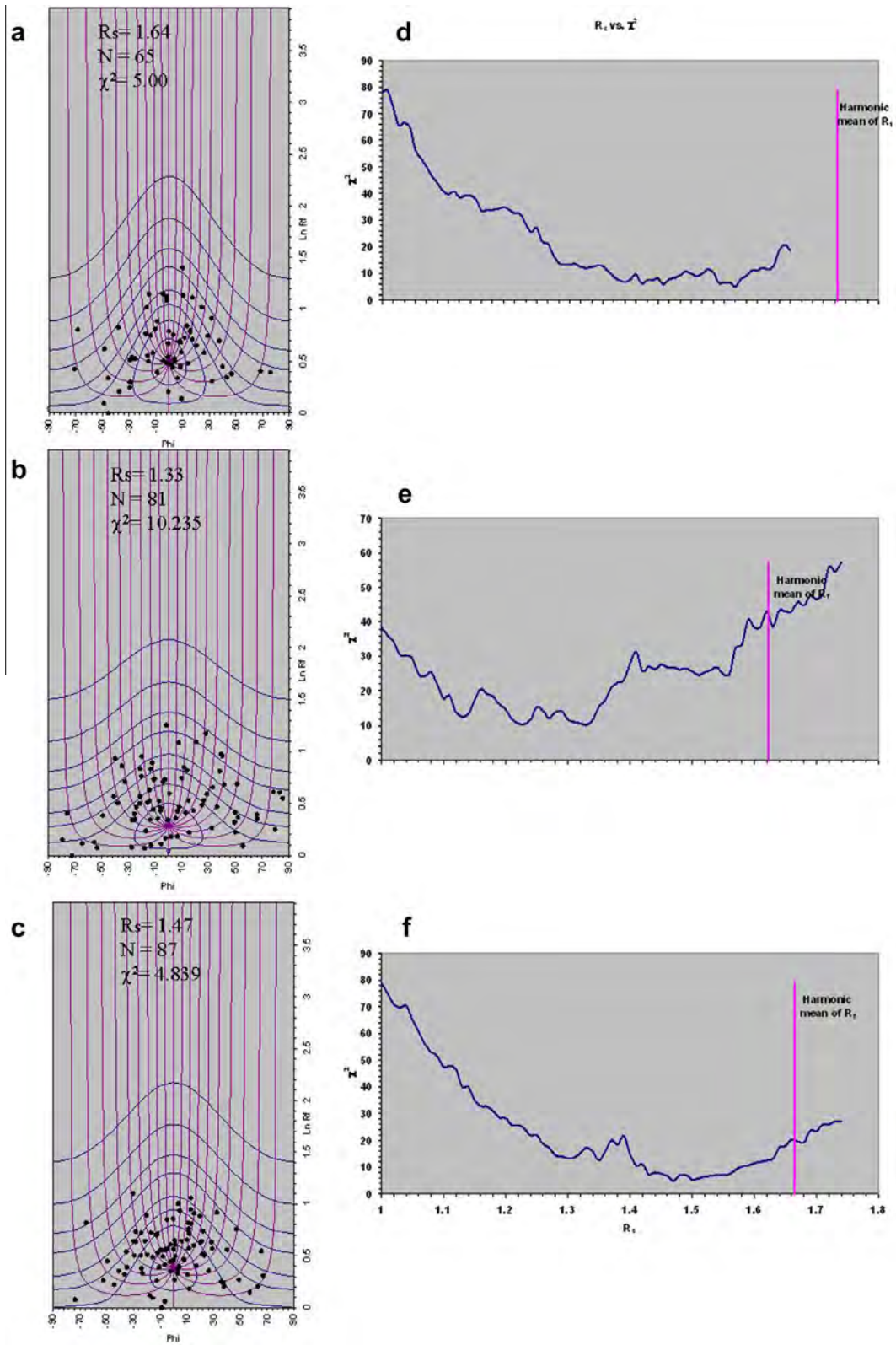


Fig. 30. (a–c) R_f/ϕ plots (after Lisle, 1985) showing the strain ratios of the deformed pebbles of the Hammamat Group exposed at Wadi Hodein. (d–f) Plotting of R_s vs. χ^2 illustrating how the best-fit parameters (χ^2) of θ -distribution text varies with strain (R_s) in the Hammamat Group exposed at Wadi Hodein.

Table 2

The Vector mean, Harmonic mean, Ln Harmonic mean and I_{SYM} for the studied post-amalgamation depositional basins obtained from CSS.

Area	Vector mean	Harmonic mean	Ln Harmonic mean	I_{SYM}
Fatima 1	-25.6215	1.8627	0.622027	0.897436
Fatima 22p	-4.6853	1.7083	0.535499	0.888889
Fatima 222p	-3.1248	1.6589	0.506155	0.873239
Fatima 66	-18.2216	1.9582	0.672026	0.911392
Fatima 400	88.6757	1.9074	0.645741	0.695652
Fatima 500	53.245	1.8694	0.625618	0.851485
Yiba 100	7.3477	1.5621	0.446031	0.859155
Yiba 101	1.2394	1.6859	0.5223	0.755556
Yiba103	-80.7315	1.9269	0.655912	0.955556
Yiba 105	-68.9526	1.6581	0.505672	0.923077
Yiba 106	87.4225	2.6692	0.981779	0.833333
Yiba 107	74.8447	1.8498	0.615078	0.953125
Um Gheig 1	2.9303	1.73	0.548121	0.927273
Um Gheig 2	-18.39	1.822	0.599935	0.869565
Um Gheig 3	4.181	1.6314	0.489439	0.857143
Um Gheig 4	18.0899	1.5649	0.447822	0.885714
Um Gheig 1	2.9303	1.73	0.548121	0.927273
Allaqi 1	32.5228	3.1577	1.149844	0.8
Allaqi 2	35.3193	1.8057	0.590948	0.595385
Allaqi 3	-44.2433	2.8217	1.03734	0.941177
Hodein 1	72.256	1.6228	0.484153	0.938272
Hodein 2	45.4793	1.8249	0.601525	0.969231
Hodein 3	8.6999	1.6646	0.509585	0.873563

Table 3

The ANOVA test and Post Hoc test (Shefee) for the studied PADBs.

	N	Mean	Std. deviation	Std. error	F	P-value
<i>Vector mean</i>						
Allaqi	3	7.8663	45.1499	26.0673	.376	.822
Fatima	6	15.0446	45.5205	18.5837		
Hodein	3	42.1451	31.9090	18.4227		
Umm Gheig	4	1.7028	15.0544	7.5272		
Yiba	6	3.5284	69.9961	28.5758		
Total	22	12.1947	46.4646	9.9063		
<i>Harmonic mean</i>						
Allaqi	3	2.5950	0.7039	0.4064	3.904	.020
Fatima	6	1.8275	0.1176	0.0480		
Hodein	3	1.7041	0.1067	0.0616		
Umm Gheig	4	1.6871	0.1127	0.0563		
Yiba	6	1.8920	0.4033	0.1646		
Total	22	1.9074	0.4203	0.0896		
<i>Ln Harmonic mean</i>						
Allaqi	3	0.9260	0.2956	0.1707	3.639	.026
Fatima	6	0.6012	0.0654	0.0267		
Hodein	3	0.5318	0.0617	0.0356		
Umm Gheig	4	0.5213	0.0666	0.0333		
Yiba	6	0.6211	0.1924	0.0785		
Total	22	0.6269	0.1885	0.0402		
<i>I_{SYM}</i>						
Allaqi	3	0.7789	0.1739	0.1004	1.220	.339
Fatima	6	0.8530	0.0798	0.0326		
Hodein	3	0.9270	0.0488	0.0282		
Umm Gheig	4	0.8849	0.0306	0.0153		
Yiba	6	0.8800	0.0788	0.0322		
Total	22	0.8661	0.0896	0.0191		

Acknowledgments

This work was funded by the Department of Structural Geology and Remote Sensing, Faculty of Earth Sciences, King Abdulaziz University, Saudi Arabia; National Authority for Remote Sensing and

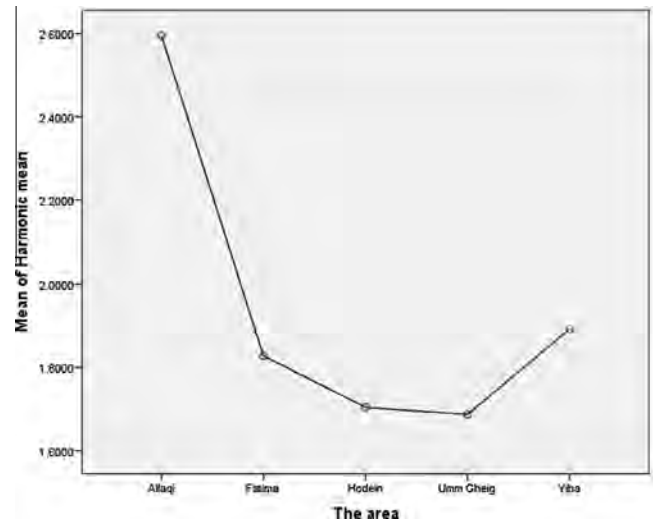


Fig. 31. The only recognized significant difference for the Harmonic mean (P -value < 0.05); a Post Hoc test (Shefee), between Allaqi and Umm Gheig areas of the HPADB.

Space Sciences (NARSS), Egypt. A serious review and comments by Prof. Y. El-Kazzaz, Helwan University, Egypt, helped greatly in improving the quality of this paper. We also benefited by discussions with Prof. M. El-Amawy and M. Abu-Anbar, Saudi Geological Survey. Special thank is extended to Prof. E. Abdelfattah, Department of Statistics, Faculty of Science, King Abdulaziz University, for his assistant in statistical tests. We would like also to thank the editors of this special issue (Prof. R.O. Greiling and A. Fowler), Dr. Ahmed Shalaby, Mansoura University, Egypt, and an anonymous reviewer for constructive comments.

References

- Abdeen, M.M., 2003. Tectonic history of the Pan-African Orogeny in Umm Gheig area, central Eastern Desert, Egypt. *Egypt Journal Geology* 47 (1), 239–254.
- Abdeen, M.M., Abdelghaffar, A.A., 2011. Syn- and post-accretionary structures in the Neoproterozoic central Allaqi-Heiani Suture Zone, Southeastern Egypt. *Precambrian Research* 185, 95–108.
- Abdeen, M.M., Dardir, A.A., Greiling, R.O., 1992. Geological and structural evolution of the Wadi Queih Area (N Quseir), Pan-African basement of the Eastern Desert of Egypt. *Zentralblatt für Geologie und Palaeontologie Teil I*, 2653–2659.
- Abdeen, M.M., Dardir, A.A., Greiling, R.O., 1997. Rain drop prints, mud crack polygons, and pebbles as strain markers in a Pan-African molasse basin, Wadi Queih, Arabian Desert, Egypt. *Annals of the Geological Survey of Egypt* 20, 185–191.
- Abdeen, M.M., Greiling, R.O., 2005. A quantitative structural study of late Pan-African compressional deformation in the Central Eastern Desert (Egypt) during Gondwana assembly. *Gondwana Research* 8, 457–471.
- Abdeen, M.M., Sadek, M.F., Greiling, R.O., 2008. Thrusting and multiple folding in the Neoproterozoic Pan-African basement of Wadi Hodein area, south Eastern Desert, Egypt. *Journal of African Earth Sciences* 52, 21–29.
- Abd El-Wahed, M.A., 2010. The role of the Najd Fault System in the tectonic evolution of the Hammamat molasse sediments, Eastern Desert, Egypt. *Arabian Journal of Geosciences*. <http://dx.doi.org/10.1007/s12517-008-0030-0>.
- Akaad, M.K., El Ramly, M.F., 1958. Seven New Occurrence of the Igla Formation in the Eastern Desert of Egypt. *The Geological Survey of Egypt Paper No. 3*, 37 p.
- Akaad, M.K., Noweir, A.M., 1969. Lithostratigraphy of the Hammamat-Umm Seleimat district, Eastern Desert of Egypt. *Nature* 223, 284–285.
- Akaad, M.K., Noweir, A.M., 1980. Geology and lithostratigraphy of the Arabian Desert orogenic belt of Egypt between latitudes 25°35' and 26°30' N. *King Abdulaziz University, Jeddah. Institute of Applied Geology Bulletin* 3 (4), 127–134.
- Al-Gabali, M.M.A., 2012. Tectonic Evolution of Wadi Fatima Fold-Thrust Belt, West-Central Part of the Arabian Shield, Saudi Arabia. M.Sc. Thesis, King Abdulaziz University, 177 p.
- Alsubhi, M.B., 2012. Geological and Structural Studies on Jabal Daf-Jabal Abu Bakr Area, Wadi Fatima, Kingdom of Saudi Arabia. M.Sc. Thesis, King Abdulaziz University, 125 p.
- Basahel, A.N., Bahafzalah, A., Omara, S., Jux, U., 1984. Early Cambrian carbonate platform of the Arabian Shield. *Neues Jahrbuch für Geologie und Paläontologie, Monatshefte (N. Jb., Geol. Paläont. Mh.)*, pp. 113–128.

- Breitkreuz, C., Eliwa, H., Khalaf, I., El Gameel, K., Bühler, B., Sergeev, S., Larionov, A., Murata, M., 2010. Neoproterozoic SHRIMP U–Pb zircon ages of silica-rich Dokhan Volcanics in the northeastern Desert, Egypt. *Precambrian Research* 182, 163–174.
- Chew, D.M., 2003. An Excel spreadsheet for finite strain analysis using the Rf/ρ technique. *Computers & Geosciences* 29, 795–799.
- Darbyshire, D.P.F., Jackson, N.J., Ramsay, C.R., Roobol, M.J., 1983. Rb–Sr isotope study of latest Proterozoic volcanosedimentary belts in the central Arabian Shield. *Journal of the Geological Society, London* 140, 203–213.
- Dardir, A.A., Abu Zeid, K.M., 1972. Geology of the basement rocks between latitudes 27°00' and 27°30' N, Eastern Desert. *Annals of the Geological Survey of Egypt* 2, 129–158.
- Davies, F.B., 1984. Strain analysis of wrench faults and collision tectonics of the Arabian–Nubian Shield. *Journal of Geology* 82, 37–53.
- Davies, F.B., 1985. Geological Map of the Al Wajh Quadrangle, Sheet 26B, Kingdom of Saudi Arabia. Saudi Arabian Deputy Ministry for Mineral Resources Geoscience Map GM 83, Scale 1:250,000, 27 p.
- Delfour, J., 1970. Le groupe de j'alah une nouvelle unite du bouchier Arabe. Bureau de Recherches Géologiques et Minières Bulletin 2 (4), 19–32.
- Dewey, J.F., 1998. Extensional collapse of orogens. *Tectonics* 7, 1123–1139.
- Donzeau, M., Benzait, P., 1989. The Ablah–Wadi Shuwas Mineral Belt–Geology and Mineral Exploration Saudi Arabian Directorate General of Mineral Resources Open File Report, B.R.G.M. OF-09-1.
- Dunnet, D., 1969. A technique of finite strain analysis using elliptical particles. *Tectonophysics* 7, 117–136.
- Duyverman, H.J., Harris, N.B.W., Hawkesworth, C.J., 1982. Crustal accretion in the Pan-African. Nd and Sr isotope evidence from the Arabian Shield. *Earth and Planetary Science Letters* 59, 315–326.
- El Ramly, M.F., 1972. A New Geological Map for the Basement Rocks in the Eastern and Southwestern Deserts of Egypt. *Annals of the Geological Survey, Egypt*, Scale 1:1,000,000, vol. 2, pp. 1–18.
- El Gaby, S., Greiling, R., 1988. The Pan-African Belt of NE Africa and Adjacent Areas, Tectonic Evolution and Economic Aspects. Vieweg, Braunschweig, Wiesbaden.
- El-Gaby, S., Khudeir, A.A., El-Taky, M., 1989. The Dokhan Volcanics of Wadi Queih area, central Eastern Desert, Egypt. In: *Proceedings of the 1st Conference on Geochemistry*. Alexandria University, Egypt, pp. 42–62.
- El-Gaby, S., List, F.K., Tehrani, R., 1988. Geology, evolution and metallogeny of the Pan-African Belt in Egypt. In: El Gaby, S., Greiling, R. (Eds.), *The Pan-African Belt of NE Africa and Adjacent Areas, Tectonic Evolution and Economic Aspects*. Vieweg, Braunschweig, Wiesbaden, pp. 17–68.
- El-Gaby, S., List, F.K., Tehrani, R., 1990. The basement complex of the Eastern Desert and Sinai. In: Said, R. (Ed.), *The Geology of Egypt*. Balkema, Rotterdam, pp. 175–184.
- Eliwa, H., Breitkreuz, C., Khalaf, I., El Gameel, K., 2010. Depositional styles of Early Ediacaran terrestrial volcanosedimentary succession in Gebel El Urf area, N Eastern Desert, Egypt. *Journal of African Earth Sciences* 57, 328–344.
- Eliwa, H.A., Kimura, J.I., Itaya, T., 2006. Late Neoproterozoic Dokhan Volcanics, N Eastern Desert, Egypt: geochemistry and petrogenesis. *Precambrian Research* 151, 31–52.
- Fritz, H., Messner, M., 1999. Intramontane basin formation during oblique convergence in the Eastern Desert of Egypt: magmatically versus tectonically induced subsidence. *Tectonophysics* 315, 145–162.
- Fritz, H., Wallbrecher, E., Khudeir, A.A., Abu El Ela, F., Dallmeyer, D.R., 1996. Formation of Neoproterozoic metamorphic core complexes during oblique convergence (Eastern Desert, Egypt). *Journal of African Earth Sciences* 23, 311–329.
- Genna, A., Guerrot, C., Deschamps, Y., Nehlig, P., Shanti, M., 1999. Les formations Ablah d'Arabie Saoudite (datation et implication géologique). *Compte Rendue Academie Sciences, Paris* 329, 661–667.
- Grainger, D.L., 2001. The late Proterozoic Fatima Group near Jeddah. *GeoArabia* 6, 103–114.
- Greenwood, W.R., 1975. Geological Map of the Jabal Ibrahim Quadrangle [20/4C]: Saudi Arabia Directorate General of Mineral Resources Geologic Map GM22.
- Greiling, R.O., Abdeen, M.M., Dadir, A.A., El Akhal, H., El Ramly, M.F., Kamal El Din, G.M., Rashwan, A.A., Rice, A.H.N., Sadek, M.F., 1994. A structural synthesis of the Proterozoic Arabian–Nubian Shield in Egypt. *Geologische Rundschau* 83, 484–501.
- Grothaus, B., Eppler, D., Ehrlich, R., 1979. Depositional environments and structural implications of the Hammamat Formation, Egypt. *Annals of the Geological Survey of Egypt* 9, 564–590.
- Hamimi, Z., El-Sawy, E.K., El-Fakharani, A., Matsah, M., Shujoon, A., El-Shafei, M.K., 2014. Neoproterozoic Structural evolution of the NE-trending 620–540 Ma Ad-Damm Shear Zone, Arabian Shield, Saudi Arabia. *Journal of African Earth Sciences* 99, 51–63.
- Hamimi, Z., El-Shafei, M., Kattu, G., Matsah, M.I., 2012a. Transpressional regime in southern Arabian Shield: insights from Wadi Yiba area, Saudi Arabia. *Mineralogy and Petrology, Special Issue Gondwana Collision*. <http://dx.doi.org/10.1007/s00710-012-0198-6>.
- Hamimi, Z., Matsah, M.I., El-Shafei, M., El-Fakharani, A., Shujoon, A., Al-Gabali, M., 2012b. Wadi Fatima thin-skinned foreland FAT belt: a post amalgamation marine basin in the Arabian Shield. *Open Journal of Geology* 2, 271–293. <http://dx.doi.org/10.4236/ojg.2012.24027>.
- Hamimi, Z., Matsah, M.I., Shujoon, A., Al-Gabali, M., 2013. The NE-Oriented Wadi Fatima Fault Zone, Near Jeddah, Saudi Arabia: A Possible Arc–Arc Suture in Western Arabian Shield. 24th Colloquium of African Geology; CAG24, Addis Ababa (Abstract).
- Hassan, M.A., Hashad, A.H., 1990. Precambrian of Egypt. In: Said, R. (Ed.), *The Geology of Egypt*. Balkema, Rotterdam, pp. 201–248.
- Johnson, P.R., 2003. Post-amalgamation basins of the NE Arabian Shield and implications for Neoproterozoic tectonism in the northern East African Orogen. *Precambrian Research* 123, 321–337.
- Johnson, P.R., Andresen, A., Collins, A.S., Fowler, A.R., Fritz, H., Ghebreab, W., Kusky, T., Stern, R.J., 2011. Late Cryogenian–Ediacaran history of the Arabian–Nubian Shield: a review of depositional, plutonic, structural, and tectonic events in the closing stages of the northern East African Orogen. *Journal of African Earth Sciences* 61, 167–232.
- Johnson, P.R., Kattan, F.H., Wooden, J.L., 2001. Implications of SHRIMP and microstructural data on the age and kinematics of shearing in the Asir Terrane, southern Arabian shield, Saudi Arabia. *Gondwana Research* 4, 172–173.
- Johnson, P.R., Woldehaimanot, B., 2003. Development of the Arabian–Nubian shield: perspectives on accretion and deformation in the northern East African Orogen and the assembly of Gondwana. In: Yoshida, M., Windley, B.F., Dasgupta, S. (Eds.), *Proterozoic East Gondwana: Supercontinent Assembly and Breakup*. The Geological Society of London, 206, Special Publication, pp. 290–325.
- Kattu, G.A.H., 2011. Structural Evolution of Wadi Yiba Area, Southern Arabian Shield, Saudi Arabia. M.Sc. Thesis, King Abdulaziz University, 140 p.
- Lisle, R.J., 1985. *Geological Strain Analysis: A Manual for the Method*. Pergamon Press, New York.
- Matsah, M.I., Kusky, T.M., 1999. Sedimentary facies of the Neoproterozoic Al-Jifn basin, NE Arabian shield: relationships to the Halaban–Zarghat (Najd) faults system and the closure of the Mozambique Ocean. In: Greiling, R. (Ed.), *Pan-African of northern Africa–Arabia*. Forschungszentrum Jülich. Geologisch Palaeontologisches Institut, Ruprecht-Karls-Universität, Heidelberg, Proceedings of a Workshop, October 22–23, 1998.
- Matsah, M.I., Kusky, T.M., 2001. Analysis of Landsat ratio imagery of the Halaban Zarghat fault and related Jifn basin, NE Arabian shield: implications for the kinematic history of the Najd fault. *Gondwana Research* 4, 182.
- Matsah, M.I., Qari, M.H.T., Hegazi, A.M., Amlas, M.A., Hamimi, Z., 2004. The Neoproterozoic Ad-Damm Shear Zone: dextral transpression in the Arabian Shield, Saudi Arabia. *Egyptian Journal of Geology* 48, 215–236.
- Mohamed, F.H., Moghazi, A.M., Hassanen, M.A., 2000. Geochemistry, petrogenesis and tectonic setting of late Neoproterozoic Dokhan-type volcanic rocks in the Fatima area, eastern Egypt. *International Journal of Earth Sciences* 88, 764–777.
- Moore T. A., Al-Rehaili, M.H., 1989. Explanatory Notes to the Geologic Map of the Makkah Quadrangle, Sheet 21-D, Geoscience Map GM-107C, Kingdom of Saudi Arabia, Ministry of Petroleum and Mineral Resources, Directorate General of Mineral Resources, 62 p.
- Moufti, M.R.H., 2001. Age, geochemistry, and origin of peraluminous A-type granitoids of the Ablah–Shuwas pluton, Ablah Graben Arabian shield. *Acta Mineralogica–Petrographica, Szeged* 2001 42, 5–20.
- Mulchrone, K.F., 2002. A statistic for estimating strain with confidence intervals from deformed line distributions with an application to schists and gneisses of the Western Gneiss Region, west central Norway. *Journal of Structural Geology* 24 (3), 545–556.
- Mulchrone, K.F., 2004. Discussion on Flattening in shear zones under constant volume: a theoretical evaluation by N. Mandal, C. Chakraborty and S. Samanta. *Journal of Structural Geology* 26 (1), 197–200.
- Mulchrone, K.F., Meere, P.A., 2001. A windows program for the analysis of tectonic strain using deformed elliptical markers. *Computers & Geosciences* 27, 1251–1255.
- Mulchrone, K.F., Meere, P.A., Choudhury, K.R., 2005. SAPE: a program for semi-automatic extraction for strain analysis. *Journal of Structural Geology* 27, 2084–2098.
- Mulchrone, K.F., O'Sullivan, F., Meere, P.A., 2003. Finite strain estimation using the mean radial length of elliptical objects with bootstrap confidence intervals. *Journal of Structural Geology* 25, 529–539.
- Nebert, K., Alshaihi, A.A., Awlia, M., Bounny, I., Nawab, Z.A., Sharief, O.H., Sherbini, O.A., Yeslam, A.H., 1974. Geology of the area north of Wadi Fatima, Kingdom of Saudi Arabia. Center for Applied Geology, Jeddah, Bulletin 1, 31p.
- Ramsay, J.G., 1967. *Folding and Fracturing of Rocks*. McGraw-Hill, New York, 531 p.
- Ressetar, R., Monrad, J.R., 1983. Chemical composition and tectonic setting of the Dokhan Volcanic formation, Eastern Desert, Egypt. *Journal of African Earth Sciences* 1, 103–112.
- Ries, A.C., Shackleton, R.M., Graham, R.H., Fitches, W.R., 1983. Pan African structures, ophiolites and mélange in the Eastern Desert of Egypt. A traverse at 26o N. *Journal of the Geological Society, London* 140, 75–95.
- Rice, A.H.N., Greiling, R.O., Dardir, A.A., Rashwan, A.A., Sadek, M.F., 1993. Pan-African extensional structures in the area S of the Hafafit Antiform, Eastern Desert of Egypt. *Zentralblatt für Geologie und Palaeontologie Teil I* 11, 2641–2651.
- Roddy, P., Purohit, M.K., Prajapati, K.K., 2010. A computer program for the determination of finite strain using Fry method. *Journal of Geological Society of India* 76, 151–154.
- Sanders, R.N., Tedder, I.J., Ford, C.R., Circosts, G., 1980. Strataform Copper Search in the Southern Ablah Group, Kingdom of Saudi Arabia: Utah Saudi Arabian Inc., Unpublished Report No.
- Sanderson, D.J., Marchini, W.R.D., 1984. Transpression. *Journal of Structural Geology* 6, 449–458.
- Shalaby, A., Stüwe, K., Fritz, H., Makroum, F., 2006. The El Mayah molasse basin in the Eastern Desert of Egypt. *Journal of African Earth Sciences* 45, 1–15.

- Stern, R.J., 1994. Arc assembly and continental collision in the Neoproterozoic East African Orogen: implications for the consolidation of Gondwanaland. *Annual Reviews of Earth and Planetary Sciences* 22, 315–319.
- Stern, R.J., Gottfried, D., Hedge, C.E., 1984. Late Precambrian rifting and crustal evolution in the northeastern Desert of Egypt. *Geology* 12, 168–172.
- Stern, R.J., Gottfried, D., 1986. Petrogenesis of a Late Precambrian (575–600 Ma) bimodal suite in the N Eastern Desert of Egypt. *Contributions to Mineralogy and Petrology* 92, 492–501.
- Stern, R.J., Hedge, C.E., 1985. Geochronologic and isotopic constraints on late Precambrian crustal evolution in the Eastern Desert of Egypt. *American Journal of Science* 285, 97–172.
- Stern, R.J., Sellers, G., Gottfried, D., 1988. Bimodal dyke swarms in the NE Desert of Egypt: significance for the origin of Late Precambrian “A-type” granites northern Afro-Arabia. In: El Gaby, S., Greiling, R. (Eds.), *The Pan-African Belt of NE Africa and Adjacent Areas, Tectonic Evolution and Economic Aspects*. Vieweg, Braunschweig, Wiesbaden, pp. 147–179.
- Tsige, L., Abdelsalam, M.G., 2005. Neoproterozoic–Early Paleozoic gravitational tectonic collapse in the southern part of the Arabian–Nubian Shield. The Balbul Belt of southern Ethiopia. *Precambrian Research* 138, 297–318.
- Wallbrecher, E., 2012. *Fabric8: A Program Package for Graphical Display and Analysis of Tectonic Data*.
- Wilde, S.A., Youssef, K., 2000. Significance of SHRIMP U–Pb dating of the imperial Porphyry and associated Dokhan Volcanics, Gebel Dokhan, N Eastern Desert, Egypt. *Journal of African Earth Sciences* 31, 410–413.
- Willis, K.M., Stern, R.J., Clauer, N., 1988. Age and geochemistry of late Precambrian sediments of the Hammamat series from the northeastern desert of Egypt. *Precambrian Research* 42, 173–187.
- Yu, H., Zheng, Y., 1984. A statistical-analysis applied to the Rf-Phi method. *Tectonophysics* 110, 151–155.
- Yihunie, T., Tesfaye, M., 2002. Structural evidence for the allochthonous nature of the Balbul terrane in southern Ethiopia: a west-verging thrust nappe. *Journal of African Earth Sciences* 34, 85–93.
- Zakir, F.A., 1972. *Geology of the Ablah Area, Southern Hijaz Quadrangle, Kingdom of Saudi Arabia*. M.Sc. Thesis, South Dakota School of Mines and Technology, 66 p.